R. & M. No. 3233

R. & M. No. 3233

MINISTRY OF AVIATION

AERONAUTICAL RESEARCH COUNCIL
REPORTS AND MEMORANDA

Generalised Methods for the Calculation of the Laminar Compressible Boundary-Layer Characteristics with Heat Transfer and Non-Uniform Pressure Distribution

By R. E. LUXTON and A. D. YOUNG

DEPARTMENT OF AERONAUTICAL ENGINEERING, QUEEN MARY COLLEGE,
UNIVERSITY OF LONDON

LONDON: HER MAJESTY'S STATIONERY OFFICE
1962
PRICE: 13*s.* 6*d.* NET

Generalised Methods for the Calculation of the Laminar Compressible Boundary-Layer Characteristics with Heat Transfer and Non-Uniform Pressure Distribution

By R. E. Luxton and A. D. Young

Department of Aeronautical Engineering, Queen Mary College, University of London

---

*Reports and Memoranda No. 3233**

January, 1960

Summary. Three related methods are presented for calculating the skin friction and other characteristics in the laminar boundary layer on a non-adiabatic wall of constant temperature in the presence of pressure gradients. The first of these methods is a direct extension of the method given by Young[5] for zero heat transfer. The assumptions made in the analysis restrict this 'first simple' method to flows with relatively small changes in free stream pressure and Mach number so that this method is applicable to the boundary layer on a thin sharp nosed wing at small angles of incidence. However, there is a need for a method of similar simplicity which can be applied to round nosed wings, that is to flows starting from a stagnation point and accelerating to supersonic velocities downstream and hence involving large changes in free stream pressure and Mach number. To meet this need the restrictive assumptions of the 'first simple' method have been relaxed and correction factors incorporated to allow for the effects of the pressure gradient on certain parameters previously assumed to be unaffected by the pressure gradient. The resulting 'complete' method involves the solution of a single quadrature in a step-by-step manner and is applicable with a high degree of accuracy to a very wide range of flows with Mach numbers from zero to five, with heat transfer to or from the surface, and with both favourable and adverse pressure gradients. For flows with favourable pressure gradients, the application of the correction factors may in part be relaxed and the 'complete' method then reduces to that which has been termed the 'second simple' method All three methods are applicable to values of the Prandtl number (σ) and the temperature-viscosity relationship index (ω) near, but not necessarily equal to, unity.

Several cases have been considered for which it is possible to compare the results given by the three methods with exact solutions and with the results given by other approximate methods. The 'complete' method is demonstrated to have advantages over other approximate methods on the grounds of accuracy, relative simplicity and breadth of application. It is also, in principle, applicable to cases with non-uniform wall temperatures although its accuracy in this application is not here examined.

---

1. *Introduction.* The majority of the methods of solution for laminar boundary layers involving both heat transfer and pressure gradients are limited by the assumption that $\omega = \sigma = 1$

* Previously issued as A.R.C. 20,336 and 21,563.

[for example, Morduchow and Grape[1], Cohen and Reshotko[2], Curle[3] and Monaghan[4]]*. However, the method developed by Young[5] for the case of zero heat transfer is generally applicable for values of ω and σ near, but not necessarily equal to, unity. This method has been extended to include heat transfer. Three methods are, in fact, presented here. The 'first simple' method is a direct extension of Young's zero heat transfer method. This method is based on a solution of the momentum equation by a single quadrature involving the assumption that H, the form factor (δ^*/θ), is independent of the local velocity, the pressure gradient, ω and σ. That is, H is assumed to be dependent only on the reference Mach number and the ratio of the wall temperature to the free stream reference temperature. It is further assumed that f, which is equal to δ_1/θ where δ_1 is the value of a transformed co-ordinate normal to the wall† corresponding to the outer edge of the boundary layer, is independent of local velocity and pressure gradient, but is dependent on the reference Mach number, the ratio of the wall temperature to the free stream reference temperature, ω and σ. A modified Pohlhausen approach is employed to obtain a second relationship between the skin friction and the momentum thickness.

The assumptions involved in the 'first simple' method restrict its application with acceptable accuracy to cases involving the types of pressure distribution likely to be found on thin wings with sharp leading edges at small incidences and Mach numbers up to about 5·0, that is, to pressure distributions with generally favourable (negative) gradients and relatively small overall variations of local free stream Mach number.

There is clearly a need for a method of similar simplicity to deal with the boundary layer on a round nosed aerofoil at supersonic speeds where the Mach number increases from zero at the forward stagnation point to supersonic values downstream. In this case the variation of the local free stream Mach number is large and hence modification of the assumptions of the 'first simple' method is required. In the 'complete' method, the parameters $H = \delta^*/\theta$ and $f = \delta_1/\theta$ are assumed to be functions of the local free stream Mach number and pressure gradient. The dependence of these parameters on the pressure gradient is achieved by reference to the set of 'similar' solutions published by Cohen and Reshotko[6] for the compressible laminar boundary layer with heat transfer and free stream velocity distributions equivalent to the power law distributions studied in incompressible flow by Falkner and Skan[7]. Simple linear correction factors have been evolved from these 'similar' solutions to correct the flat plate values of H and f for the effects of pressure gradient. The resulting 'complete' method is of a high order of accuracy and can be applied to a very wide range of cases from strong adverse to strong favourable pressure gradients including the case of flow from a forward stagnation point. Not only is the skin-friction distribution predicted accurately by the 'complete' method, but the distributions of the momentum and displacement thicknesses are similarly predicted. This is of importance for the calculation of the second order contribution to the drag on aerofoils due to the interaction between the boundary layer and the free stream[8].

The 'complete' method requires the calculation of a single quadrature in a step-by-step manner. However, for relatively small favourable pressure gradients it may be usefully shortened to yield a 'second simple' method. This method is preferred to the 'first simple' method for this class of problems, as it is rather more general in its formulation and may easily be extended to the 'complete' method if this should prove necessary.

---

* Since this paper was prepared Curle[10] has generalised his method to deal with values of ω and σ other than unity.

† Defined in Section 2.

It is relevant here to examine briefly other methods that have been developed and with which the methods of this paper are later compared. These alternative methods apply only to the case when $\omega = \sigma = 1$.

Cohen and Reshotko[2], from their set of 'similar' solutions, have evaluated a shear parameter, a correlation number, and a heat transfer parameter, in a manner analogous to that used by Thwaites[9] for zero heat transfer in incompressible flow, and have reduced the solution of the momentum equation for the evaluation of the skin friction to a single quadrature by the formulation of a unique correlation between these parameters. The method is simple to apply and yields reasonable results. It is, however, limited by the range and accuracy of the set of 'similar' solutions on which it is based and these solutions are only for relatively small favourable to strong adverse pressure gradients. Further, as the flow approaches separation in an adverse pressure gradient the correlation number reaches a maximum and then begins to decrease. As a consequence, it is not possible to predict the separation point accurately.

A basic difference between the 'complete' method of this paper and the method of Cohen and Reshotko is that the former uses the 'similar' solutions only to provide small correction factors, whereas the latter is completely dependent on the 'similar' solutions and so its validity for cases very different from those solutions is open to some doubt.

Curle[2] assumed that the temperature is a quadratic function of the velocity and transformed the momentum equation by a Howarth transformation. The solution is obtained by an adaptation of Thwaites' method. The computation involves a double quadrature.

A representative range of cases have been considered for which it is possible to compare the results given by the methods of this paper, and by the other methods, with exact solutions. The comparisons indicate that the 'complete' method yields the most reliable results.

The general effects of heat transfer and pressure gradient on the skin friction are discussed in the light of these detailed calculations and simple physical arguments are offered to explain them.

2. *'First Simple' Method.* The following analysis is an extension of the analysis for the zero heat transfer case as presented by Young[5]. Suffix *a* will be used to denote the reference conditions just aft of the leading-edge shock, if any, and suffix 1 will be used to denote the local values just outside the boundary layer.

The momentum equation of the boundary layer is

$$\theta' + \left[(H+2)\frac{u_1'}{u_1} + \frac{\rho_1'}{\rho_1}\right]\theta = \frac{\tau_w}{\rho_1 u_1^2} \tag{1}$$

where accents denote differentiation with respect to x, the distance along the surface, and

$H = \frac{\delta^*}{\theta}$, where $\delta^* = \int_0^\infty \left(1 - \frac{\rho u}{\rho_1 u_1}\right) dy$, is the displacement thickness

and $\theta = \int_0^\infty \frac{\rho u}{\rho_1 u_1}\left(1 - \frac{u}{u_1}\right) dy$, is the momentum thickness, all other symbols being defined in the Notation.

Instead of expressing a Pohlhausen velocity distribution as a function of y, it will be expressed, in accordance with Equation (24) of Ref. 5, as a function of $Y = \int_0^y \frac{\mu_a}{\mu}\, dy$ since this function is likely to be much less dependent on Mach number. Suppose the velocity distribution across the boundary layer to be given by the quartic

$$u = aY + bY^2 + cY^3 + dY^4 \tag{2}$$

with the boundary conditions that for

$$Y = \delta_1,\ u = u_1,\ \frac{\partial u}{\partial Y} = \frac{\partial^2 u}{\partial Y^2} = 0,$$

and for

$$Y = 0,\ u = 0,\ T = T_w \text{ and hence } \mu = \mu_w.$$

The quantity δ_1 is unknown but is taken to be the value of Y which corresponds to the value of y defining the outer edge of the boundary layer.

The first boundary-layer equation yields

$$\frac{\partial}{\partial y}\left(\mu \frac{\partial u}{\partial y}\right)_w = \frac{dp}{dx} = -\rho_1 u_1 u_1'.$$

But

$$\frac{\partial u}{\partial y} = \frac{\partial u}{\partial Y}\frac{\partial Y}{\partial y} = \frac{\mu_a}{\mu}\frac{\partial u}{\partial Y},$$

and hence

$$\frac{\partial}{\partial y}\left[\mu \frac{\partial u}{\partial y}\right]_w = \frac{\partial}{\partial y}\left[\mu_a \frac{\partial u}{\partial Y}\right]_w = \frac{\mu_a^2}{\mu_w}\left[\frac{\partial^2 u}{\partial Y^2}\right]_w.$$

Therefore

$$\frac{\mu_a^2}{\mu_w}\left(\frac{\partial^2 u}{\partial Y^2}\right)_w = -\rho_1 u_1 u_1'. \tag{3}$$

With these boundary conditions we can solve for a, b, c, d in (2) in terms of δ_1, and this yields

$$\left.\begin{aligned} a &= \frac{u_1(12+\Lambda)}{6\delta_1}, \quad b = -\frac{u_1\Lambda}{2\delta_1^2}, \quad c = -\frac{u_1(4-\Lambda)}{2\delta_1^3}, \\ d &= \frac{u_1(6-\Lambda)}{6\delta_1^4}, \quad \text{where } \Lambda = u_1'\delta_1^2\rho_1\frac{\mu_w}{\mu_a^2}. \end{aligned}\right\} \tag{4}$$

Further, since

$$\tau_w = \mu_w\left(\frac{\partial u}{\partial y}\right)_w = \mu_a\left(\frac{\partial u}{\partial Y}\right)_w = \mu_a a,$$

then

$$\frac{\tau_w}{\rho_1 u_1^2} = \frac{\mu_a(12+\Lambda)}{6\delta_1\rho_1 u_1}. \tag{5}$$

The method now departs from the classical Pohlhausen approach. It depends on the solution of the momentum equation, using the following assumptions:

(i) Equation (5) is accepted.

(ii) The variation of H with the local velocity, pressure gradient, ω and σ is neglected where ω is the temperature-viscosity relationship index and σ is the Prandtl number. H is then treated as a function of M_a and T_w/T_a only. The justification for this lies in the fact that H enters the solution of the momentum equation in a form which suggests that the solution is relatively insensitive to small variations of H, and for thin wings at small incidences the possible variations of H are unlikely to be large.

(iii) The ratio δ_1/θ is also assumed to be independent of local velocities and pressure gradient, and for the present we write

$$\frac{\delta_1}{\theta} = f\left(M_a, \frac{T_w}{T_a}, \omega, \sigma\right) \tag{6}$$

making no further assumptions at this stage about the form of the function other than noting that we expect it to be constant when ω is unity.

With regard to assumption (ii), for a flat plate at zero incidence with $\omega = 1$, we know that u/u_a is a unique function of Y. For a flat plate at zero incidence, $u_1 = u_a$, $T_1 = T_a$, etc. Hence

$$\theta = \int_0^\infty \frac{\rho u}{\rho_a u_a}\left(1 - \frac{u}{u_a}\right) dy = \int_0^\infty \frac{u}{u_a}\left(1 - \frac{u}{u_a}\right) dY = \theta_{i,0} \tag{7}$$

where suffix $i,0$ denotes the value in incompressible flow and with zero heat transfer, also

$$\delta^* = \int_0^\infty \left(1 - \frac{\rho u}{\rho_a u_a}\right) dy = \int_0^\infty \left(\frac{\mu}{\mu_a} - \frac{u}{u_a}\right) dY.$$

But $\dfrac{\mu}{\mu_a} = \dfrac{T}{T_a} = i$ for a perfect gas with constant specific heats where $i = \dfrac{I}{I_1} = \dfrac{I}{I_a} =$ ratio of enthalpies. Now using the notation of $\eta = u/u_1$, $i = I/I_1$, and Crocco's transformation, from Equation (22) of Ref. 5, we have for $\sigma = 1 \cdot 0$

$$i = i(0) + \left[1 - i(0) + \frac{u_1^2}{2I_1}\right]\eta - \frac{u_1^2}{2I_1}\eta^2 \tag{8}$$

where

$$i(0) = \frac{I_w}{I_1} = \frac{I_w}{I_a} = \frac{T_w}{T_a}.$$

But

$$\frac{u_1^2}{2I_1} = \frac{u_1^2}{2c_p T_1} = \frac{u_1^2(\gamma - 1)\rho_1}{2\gamma p_1}$$

$$= \frac{(\gamma - 1)}{2} M_1^2.$$

Hence in (8)

$$i = i(0) + \left[1 - i(0) + \frac{(\gamma - 1)}{2} M_1^2(1 - \eta)\right]\eta.$$

Therefore

$$\delta^* = \int_0^\infty \left(\frac{\mu}{\mu_1} - \frac{u}{u_1}\right) dY = \int_0^\infty \left[i(0)(1 - \eta) + \frac{(\gamma - 1)}{2} M_1^2(1 - \eta)\eta\right] dY,$$

thus

$$\delta^* = i(0)\delta^*_{i,0} + \frac{(\gamma - 1)}{2} M_1^2 \theta_{i,0}, \tag{9}$$

and

$$H = \frac{\delta^*}{\theta} = i(0)H_{i,0} + \frac{\gamma - 1}{2} M_1^2$$

i.e.,

$$H = \frac{T_w}{T_1} H_{i,0} + \frac{\gamma - 1}{2} M_1^2 \tag{10}$$

where $H_{i,0}$ denotes the value of H in incompressible flow with zero heat transfer. The Blasius solution gives

$$H_{i,0} = 2 \cdot 59 .$$

Hence

$$H = 2 \cdot 59 \frac{T_w}{T_1} + 0 \cdot 2 M_1^2 \tag{11}$$

for

$$\gamma = 1 \cdot 4 .$$

From Equation (5) and the expression for Λ in (4)

$$\begin{aligned} \frac{\tau_w}{\rho_1 u_1^2} &= \frac{\mu_a}{6 \rho_1 u_1 \delta_1} \left[12 + u_1' \delta_1^2 \rho_1 \frac{\mu_w}{\mu_a^2} \right] \\ &= \frac{12 \mu_a}{6 \rho_1 u_1 \delta_1} + \frac{u_1' \delta_1 \mu_w}{6 u_1 \mu_a} \\ &= \frac{2 \mu_a}{\rho_1 u_1 f \theta} + \frac{u_1'}{6 u_1} \frac{\mu_w}{\mu_a} f \theta . \end{aligned}$$

Hence the momentum equation (1) becomes

$$\theta' + \left[(H+2) \frac{u_1'}{u_1} + \frac{\rho_1'}{\rho_1} \right] \theta = \frac{u_1'}{6 u_1} \frac{\mu_w}{\mu_a} f \theta + \frac{2 \mu_a}{\rho_1 u_1 f \theta} .$$

Multiplying both sides by $2 \rho_1^2 \theta$, we get

$$\frac{d}{dx} [\rho_1^2 \theta^2] + 2 \rho_1^2 \theta^2 \frac{u_1'}{u_1} \left[(H+2) - \frac{f}{6} \frac{\mu_w}{\mu_a} \right] = \frac{4 \mu_a \rho_1}{u_1 f} . \tag{12}$$

Now $\frac{\mu_w}{\mu_a} = \left(\frac{T_w}{T_a} \right)^w$ and we write $\left[(H+2) - \frac{f}{6} \frac{\mu_w}{\mu_a} \right] = \frac{g}{2}$

where g is a function of M_a, $\frac{T_w}{T_a}$, ω, σ, (13)

and is constant for a particular boundary layer.

Equation (12) then integrates to

$$\left[u_1^g \rho_1^2 \theta^2 \right]_0^{x_1} = 4 \mu_a \int_0^{x_1} \frac{\rho_1 u_1^{g-1}}{f} dx . \tag{14}$$

The leading edge is taken as $x = 0$, where either $u = 0$ or u_1 is finite. If u_1 is finite at the leading edge then $\theta = 0$, since we cannot have a finite momentum loss there. Hence

$$\left[\rho_1^2 \theta^2 \right]_{x_1} = \frac{4 \mu_a}{[u_1]_{x_1}^g} \int_0^{x_1} \frac{\rho_1 u_1^{g-1}}{f} dx . \tag{15}$$

Notice here that g occurs as an exponent of u_1 both inside the integral and in the denominator outside the integral. This suggests that provided the variation of u_1 with x is small, small errors in

g will have little effect, and this provides some justification for the neglect of the variation of H with pressure gradient and local velocity. We must now determine the function f. For a flat plate at zero incidence (15) reduces to

$$\left[\rho_a \theta^2\right]_{x_1} = \frac{4\mu_a}{f u_a} x_1$$

or

$$\frac{\theta\sqrt{R_x}}{2x} = \sqrt{\frac{1}{f}} \quad \text{where } R_x = \frac{u_a \rho_a x}{\mu_a}$$

and

$$\frac{\partial\theta}{\partial x} = \frac{1}{\sqrt{R_x f}}.$$

But

$$c_f = \frac{2\tau_w}{\rho_a u_a^2} = 2\frac{\partial\theta}{\partial x} = \frac{2}{\sqrt{R_x f}}.$$

Now Equation (36) of Ref. 5 gives

$$c_f\sqrt{R_x} = 0\cdot 664\,[0\cdot 45 + 0\cdot 55 i(0) + 0\cdot 09(\gamma-1)M_1^2\sigma^{1/2}]^{(\omega-1)/2}. \tag{16}$$

Therefore

$$c_f\sqrt{R_x} = \frac{2}{\sqrt{f}} = 0\cdot 664\,[0\cdot 45 + 0\cdot 55 i(0) + 0\cdot 09(\gamma-1)M_1^2\sigma^{1/2}]^{(\omega-1)/2}$$

or

$$f = 9\cdot 072\,[0\cdot 45 + 0\cdot 55 i(0) + 0\cdot 09(\gamma-1)M_1^2\sigma^{1/2}]^{1-\omega}. \tag{17}$$

The function g is given by

$$g = 2(H+2) - \frac{f}{3}\frac{\mu_w}{\mu_a}$$

$$= 5\cdot 18\frac{T_w}{T_a} + 0\cdot 4M_a^2 + 4 - 3\cdot 024\left[0\cdot 45 + 0\cdot 55\frac{T_w}{T_a} + 0\cdot 036 M_a^2\sigma^{1/2}\right]^{1-\omega}\left(\frac{T_w}{T_a}\right)^{w}, \tag{18}$$

as $M_1 = M_a$ for a flat plate.

It is convenient to express these relations in non-dimensional form. Then (15) becomes

$$\left[\left(\frac{\rho_1}{\rho_a}\right)^2\left(\frac{\theta}{L}\right)^2 R_L\right]_{x_1/L} = \frac{4}{(u_1/u_a)_{x_1/L}^{g}}\int_0^{x_1/L}\frac{1}{f}\frac{\rho_1}{\rho_a}\left(\frac{u_1}{u_a}\right)^{g-1} d(x/L), \tag{19}$$

where

$$R_L = \frac{\rho_a u_a L}{\mu_a}.$$

The isentropic relationship between ρ_1 and u_1 is, non-dimensionally

$$\frac{\rho_1}{\rho_a} = \left[1 + \frac{(\gamma-1)}{2}M_a^2\left\{1 - \left(\frac{u_1}{u_a}\right)^2\right\}\right]^{1/(\gamma-1)}. \tag{20}$$

Having u_1 as a function of x, we can obtain θ at any point from Equations (17), (18), (19) and (20), the solution of (19) being obtained by graphical or numerical integration.

To obtain the local skin-friction coefficient when θ is known, we have

$$c_f = \frac{2\tau_w}{\rho_a u_a^2} = \frac{(12+\Lambda)\dfrac{u_1}{u_a}}{3f\dfrac{\theta}{L}R_L} \tag{21}$$

where

$$\Lambda = u_1'\delta_1^2\rho_1\frac{\mu_w}{\mu_a^2}$$

$$= \frac{u_1'L}{u_a}f^2\left(\frac{\theta}{L}\right)^2 R_L\frac{\rho_1}{\rho_a}\frac{\mu_w}{\mu_a}, \tag{22}$$

and

$$\frac{\mu_w}{\mu_a} = \left(\frac{T_w}{T_a}\right)^\omega.$$

Hence

$$c_f\sqrt{R_x} = \frac{\dfrac{u_1}{u_a}\left(12+\Lambda\right)\left(\dfrac{x}{L}\right)^{1/2}}{3f\dfrac{\theta}{L}\sqrt{R_L}} \tag{23}$$

$$= \frac{\dfrac{u_1}{u_a}\left(12+\Lambda\right)\left(\dfrac{x}{L}\right)^{1/2}}{3\left(\Lambda\Big/\dfrac{\rho_1}{\rho_a}\dfrac{u_1'L}{u_a}\dfrac{\mu_w}{\mu_a}\right)^{1/2}}. \tag{24}$$

It will be seen from Equation (19) that this method involves only a single quadrature and, therefore, is easily computed. The method is applicable with acceptable accuracy to cases involving the types of pressure distribution likely to be found on thin wings with sharp leading edges at small incidences and Mach numbers up to about five; that is, pressure distributions with generally favourable (negative) gradients with respect to the streamwise direction, and relatively small overall variations of local free stream Mach number.

However, as remarked in the Introduction, there is a need for a method of similar simplicity to deal with the boundary layer on a round nosed wing section at supersonic speeds where the Mach number increases from zero at the forward stagnation point to supersonic values downstream. To deal with this class of problem modification is required of the assumptions that the parameters f and H are constant in each case, and are functions only of the initial flow conditions just aft of the leading-edge shock wave and are independent of the pressure gradient. In the light of the series of exact 'similar' solutions evaluated by Cohen and Reshotko[2], it has been found readily possible to make the required modifications, and in particular, the boundary-layer parameters f and H can be presented as functions of the local free stream conditions and of the pressure gradient. With these modifications the 'first simple' method has been generalized to deal with any type of pressure distribution, with no restriction on the range of variation of local free stream Mach number, and is now presented as the 'complete' method following a discussion of the effect of pressure gradient on the parameters f and H.

3. *The Influence of Pressure Gradient on the Parameters f and H.* 3.1. *The Parameter* $f = \delta_1/\theta$. In the previous section the velocity in the boundary layer was expressed as a quartic in Y where

$$Y = \int_0^y \frac{\mu_a}{\mu}\, dy\,,$$

y being the distance normal to the surface, and suffix a referring to a reference point in the free stream just aft of the leading-edge shock. Since the main concern here is with problems involving a much wider range of local free stream conditions, including possible stagnation conditions at the leading edge, this definition of Y becomes unsuitable and it is modified to

$$Y = \int_0^y \frac{\mu_1}{\mu}\, dy\,, \tag{25}$$

where suffix 1 refers to local free stream values just outside the boundary layer. The quantity δ_1 is then defined as the value of Y corresponding to the value of y defining the outer edge of the boundary layer.

It was shown in the previous section that on a flat plate at zero incidence, the parameter $f = \delta_1/\theta$ (where θ is the momentum thickness) is given by

$$f = f_{f.p.} = 9\cdot072 \left[0\cdot45 + 0\cdot55\frac{T_w}{T_1} + 0\cdot09(\gamma-1)\, M_1^2\sigma^{1/2}\right]^{1-\omega}. \tag{26}$$

It was then assumed in the 'first simple' method that f was independent of the free stream pressure gradient. However, in the presence of strong pressure gradients, particularly if they are adverse, the change in the shape of the velocity profile due to the pressure gradient makes f a slowly varying function of the pressure gradient. To allow for this variation, the functional relationship between f and a non-dimensional pressure gradient parameter is sought. A convenient parameter is Λ which, when allowance is made in Equation (22) for the different transformation of the y cordinate, becomes

$$\Lambda = -\frac{dp}{dx}\frac{\delta_1^2}{u_1}\frac{\mu_w}{\mu_1^2} = \frac{du_1}{dx}\,\delta_1^2\rho_1\frac{\mu_w}{\mu_1^2}. \tag{27}$$

Cohen and Reshotko[2] have presented curves of l as a function of n, where l and n are the compressible flow counterparts of Thwaites' parameters l and m. For these calculations the parameters ω and σ were unity. l is defined as

$$l = \frac{\theta}{u_1}\frac{T_w}{T_1}\left(\frac{du}{dy}\right)_w. \tag{28}$$

Now

$$\tau_w = \mu_w\left(\frac{du}{dy}\right)_w$$

and with the assumption of a quartic velocity distribution this becomes

$$\tau_w = \frac{\mu_1(12+\Lambda)u_1}{6f\theta}.$$

Hence, with $\omega = 1\cdot0$, we find

$$l = \frac{(12+\Lambda)}{6f}. \tag{29}$$

Also n is defined as

$$n = -\frac{du_1}{dx}\frac{\theta^2}{\nu_w}\left(\frac{T_w}{T_1}\right)^2\left(\frac{T_0}{T_1}\right) \tag{30}$$

$$= -u_1'\theta^2\frac{\rho_1}{\mu_1}\frac{T_0}{T_1}, \text{ for } \omega = 1\cdot 0.$$

But

$$\Lambda = u_1' f^2\theta^2\rho_1\frac{\mu_w}{\mu_1^2}, \text{ by Equation (27)},$$

hence

$$\left.\begin{aligned} n &= -\frac{\Lambda}{f^2}\frac{T_0}{T_w} \\ \Lambda &= -nf^2\frac{T_w}{T_0}. \end{aligned}\right\} \tag{31}$$

or

Therefore

$$l = \left(12 - nf^2\frac{T_w}{T_0}\right)\Big/ 6f \tag{32}$$

Hence

$$f = \frac{-6l + \sqrt{\{36l^2 + 48n(1+S_w)\}}}{2n(1+S_w)}, \tag{33}$$

where S_w is defined by

$$S_w = \frac{T_w}{T_r} - 1.$$

T_r is the recovery temperature, assumed to be given by

$$\frac{T_r}{T_1} = \left[1 + \frac{\gamma - 1}{2}M_1^2\sigma^{1/2}\right], \tag{34}$$

and $T_r = T_0$ for $\sigma = 1\cdot 0$.

Thus, from the Cohen and Reshotko plots of l as a function of n for various values of S_w, f may be determined as a function of Λ for various values of S_w. These functions are presented in Figure 2. A simple correction to f to allow for the effect of pressure gradient is sought, and these curves suggest a linear approximation to the relation between f and Λ in the form

$$f = f_{f.p.}(1 + k_1\Lambda), \tag{35}$$

where

$$f_{f.p.} = \left[\frac{\delta_1}{\theta}\right]_{\Lambda=0},$$

and the factor k_1 is shown as a function of S_w in Figure 3. It will be noticed that k_1 is negative.

The factor k_1 is small for positive and small negative values of S_w, *i.e.*, for heat transfer from the surface to the fluid or for small heat transfer rates to the surface, but for large negative values of S_w (high heat transfer rates to the surface) the correction on f due to the pressure gradient can become important, particularly with an adverse pressure gradient where $|\Lambda|$ is large. Although the curves of Figures 2 and 3 are derived from calculations for $\omega = \sigma = 1$, it is assumed that for the purposes of correcting f for pressure gradient effects they are applicable where ω and σ are near unity.

3.2. *The Form Factor* $H = \delta^*/\theta$. It was shown earlier, Equation (10), that for a flat plate at zero incidence the parameter H was given by

$$H_{f.p.} = \frac{T_w}{T_1} H_{i,0} + \frac{\gamma - 1}{2} M_1^2. \tag{36}$$

In terms of S_w and Mach number (36) becomes

$$H_{f.p.} = \left[(1+S_w)H_{i,0}\right]\left(1 + \frac{\gamma - 1}{2} M_1^2 \sigma^{1/2}\right) + \frac{\gamma - 1}{2} M_1^2 \tag{37}$$

Cohen and Reshotko[6] write

$$H = H_{tr.}\left(1 + \frac{\gamma - 1}{2} M_1^2\right) + \frac{\gamma - 1}{2} M_1^2, \tag{38}$$

where $H_{tr.}$ is a transformed form factor.

The form of (38) is similar to that of (37) for unit Prandtl number. If, therefore, on the basis of Cohen and Reshotko's solutions, the factors $(1+S_w)H_{i,0}$ and $H_{tr.}$ can be related by some term involving the pressure gradient, Equation (37) may be corrected to allow for the effect of pressure gradient.

Write, for $\sigma = 1 \cdot 0$

$$H = \left[(1+S_w)H_{i,0} + \phi(\Lambda)\right]\left(1 + \frac{\gamma - 1}{2} M_1^2\right) + \frac{\gamma - 1}{2} M_1^2,$$

then

$$\phi(\Lambda) = H_{tr.} - (1+S_w)H_{i,0}. \tag{39}$$

This function has been evaluated from the similar solutions of Cohen and Reshotko[2] for various values of S_w and is plotted in Figure 4.

For cooled walls the relationship is almost linear, and therefore it is approximately

$$\phi(\Lambda) = k_2 \Lambda.$$

Hence, the expression for H becomes

$$H = \left[(1+S_w)H_{i,0} + k_2\Lambda\right]\left(1 + \frac{\gamma - 1}{2} M_1^2 \sigma^{1/2}\right) + \frac{\gamma - 1}{2} M_1^2. \tag{40}$$

The relationship between k_2 and S_w is plotted in Figure 5. It should be noted that as defined k_2 is independent of the Mach number and therefore the pressure gradient effect on H may be examined separately from the influence of Mach number.

4. *The 'Complete' Method.* The development of the complete method now follows similar lines to those of the 'first simple' method. The momentum equation of the boundary layer is

$$\theta' + \left[(H+2)\frac{u_1'}{u_1} + \frac{\rho_1'}{\rho_1}\right]\theta = \frac{\tau_w}{\rho_1 u_1^2}. \tag{41}$$

The velocity profile is assumed to be of the form

$$u = aY + bY^2 + cY^3 + dY^4 \tag{42}$$

where Y is given by Equation (25) and a, b, c, d are constants.

The boundary conditions are

$$Y = \delta_1, \qquad u = u_1, \qquad \frac{\partial u}{\partial Y} = \frac{\partial^2 u}{\partial Y^2} = 0;$$

$$Y = 0, \qquad u = 0, \qquad T = T_w,$$

where δ_1 is the value of Y which corresponds to the value of y defining the outer edge of the boundary layer.

The first boundary-layer equation yields

$$\frac{\partial}{\partial y}\left(\mu\frac{\partial u}{\partial y}\right)_w = \frac{dp}{dx} = -\rho_1 u_1 u_1'.$$

But

$$\frac{\partial u}{\partial y} = \frac{\partial u}{\partial Y}\frac{\partial Y}{\partial y} = \frac{\mu_1}{\mu}\frac{\partial u}{\partial Y}$$

and hence

$$\frac{\partial}{\partial y}\left[\mu\frac{\partial u}{\partial y}\right]_w = \frac{\partial}{\partial y}\left[\mu_1\frac{\partial u}{\partial Y}\right]_w = \frac{\mu_1^2}{\mu_w}\left[\frac{\partial^2 u}{\partial Y^2}\right]_w.$$

Therefore

$$\frac{\mu_1^2}{\mu_w}\left(\frac{\partial^2 u}{\partial Y^2}\right)_w = -\rho_1 u_1 u_1'. \tag{43}$$

From the boundary conditions and Equation (43) we obtain for a, b, c, d in Equation (42)

$$\left.\begin{aligned} a &= \frac{u_1(12+\Lambda)}{6\delta_1}, \qquad b = -\frac{u_1\Lambda}{2\delta_1^2}, \qquad c = -\frac{u_1(4-\Lambda)}{2\delta_1^3}, \\ d &= \frac{u_1(6-\Lambda)}{6\delta_1^4}, \qquad \text{where } \Lambda = u_1'\delta_1^2\rho_1\frac{\mu_w}{\mu_1^2}. \end{aligned}\right\} \tag{44}$$

However

$$\tau_w = \mu_w\left(\frac{\partial u}{\partial y}\right)_w = \mu_1\left(\frac{\partial u}{\partial Y}\right)_w = \mu_1 a.$$

Therefore

$$\frac{\tau_w}{\rho_1 u_1^2} = \frac{\mu_1(12+\Lambda)}{6\delta_1\rho_1 u_1}. \tag{45}$$

Equation (41) is now considered over a suitable range of x from x_n to x_{n+1}, say. The expression for H is given by Equation (40), and, substituting the Blasius incompressible value of $H_{i,0} = 2\cdot59$, this becomes

$$H = \left[2\cdot59(1+S_w) + k_2\Lambda\right]\left(1 + \frac{\gamma-1}{2}M_1^2\sigma^{1/2}\right) + \frac{\gamma-1}{2}M_1^2 \tag{46}$$

We write, Equation (35),

$$\delta_1/\theta = f = f_{f.p.}(1+k_1\Lambda)$$

and we assume $f_{f.p.}$ is the function of M_1, $\frac{T_w}{T_1}$, ω and σ defined in Equation (17).

Rewriting Equation (45) with $\delta_1 = f\theta$ we have

$$\begin{aligned} \frac{\tau_w}{\rho_1 u_1^2} &= \frac{\mu_1}{6\rho_1 u_1 f\theta}\left[12 + u_1' f^2\theta^2\rho_1\frac{\mu_w}{\mu_1^2}\right] \\ &= \frac{2\mu_1}{\rho_1 u_1 f\theta} + \frac{u_1'\mu_w}{6u_1\mu_1}f\theta. \end{aligned} \tag{47}$$

Therefore, Equation (41) becomes

$$\theta' + \theta\left[(H+2)\frac{u_1'}{u_1} + \frac{\rho_1'}{\rho_1}\right] = \frac{u_1'}{6u_1}\frac{\mu_w}{\mu_1}f\theta + \frac{2\mu_1}{\rho_1 u_1 f\theta}. \tag{48}$$

Multiplying Equation (48) by $2\rho_1{}^2\theta$ we obtain

$$\frac{d}{dx}\left[\rho_1{}^2\theta^2\right] + 2\rho_1{}^2\theta^2\frac{u_1'}{u_1}\left[(H+2) - \frac{f}{6}\frac{\mu_w}{\mu_1}\right] = \frac{4\mu_1\rho_1}{u_1 f}. \tag{49}$$

We now write

$$\left[(H_n+2) - \frac{f_n}{6}\frac{\mu_w}{\mu_1}\right] = \frac{g_n}{2}, \tag{50}$$

where H_n and f_n are assumed constant over the range of x from x_n to x_{n+1}; μ_w/μ_1 is also taken as constant over this range and is given by

$$\frac{\mu_w}{\mu_1} = \left(\frac{T_w}{T_1}\right)^\omega \text{ at } x_n, \tag{51}$$

where ω is the index of the temperature-viscosity relationship.

Thus g_n is assumed constant over the range x_n to x_{n+1}. Equation (49) may now be integrated over the range x_n to x_{n+1} to give

$$\left[\rho_1{}^2\theta^2 u_1{}^{g_n}\right]_{x_n}^{x_{n+1}} = 4\int_{x_n}^{x_{n+1}} \frac{\rho_1\mu_1 u_1{}^{(g_n-1)}}{f_n}\,dx. \tag{52}$$

We again note that g_n occurs in (52) in such a manner that provided the variation of u_1 with x is reasonably small over the range of the integration, the value of θ obtained from (52) is relatively insensitive to the value of g_n. Thus, for cases involving small variations of free stream Mach number, larger integration steps may be taken than for cases involving large variations of free stream Mach number.

In non-dimensional form Equation (52) is

$$\left.\begin{aligned} &\left[\left(\frac{\rho_1}{\rho_a}\right)^2\left(\frac{\theta}{L}\right)^2 R_L\right]_{n+1} - \left[\left(\frac{\rho_1}{\rho_a}\right)^2\left(\frac{\theta}{L}\right)^2 R_L\right]_n \frac{[(u_1/u_a)^{g_n}]_n}{[(u_1/u_a)^{g_n}]_{n+1}} \\ &\qquad = \frac{4}{\left[\left(\dfrac{u_1}{u_a}\right)^{g_n}\right]_{n+1}} \int_{x_n/L}^{x_{n+1}/L} \frac{\left(\dfrac{\rho_1}{\rho_a}\right)\left(\dfrac{\mu_1}{\mu_a}\right)\left(\dfrac{u_1}{u_a}\right)^{(g_n-1)}}{f_n}\,d\left(\frac{x}{L}\right), \end{aligned}\right\} \tag{53}$$

where suffix a signifies some reference condition to be defined, L is some representative length which may be related to the chord, and

$$R_L = \frac{\rho_a u_a L}{\mu_a} \text{ as before.}$$

The quadrature on the right hand side of Equation (53) may be evaluated numerically or graphically and a value of $\frac{\theta}{L}\sqrt{R_L}$ obtained at the point x_{n+1}.

From Equation (44) the pressure gradient parameter Λ may now be found. Expressed in non-dimensional terms, (44) becomes

$$\Lambda = \frac{u_1'L}{u_a}\frac{\rho_1}{\rho_a}\frac{\mu_w}{\mu_a}\left(\frac{\mu_a}{\mu_1}\right)^2 f^2 \left(\frac{\theta}{L}\right)^2 R_L. \tag{54}$$

To evaluate this expression at the point x_{n+1} the value of $\left[\left(\frac{\theta}{L}\right)^2 R_L\right]_{n+1}$ obtained from Equation (53) and the value of f_n at x_n is used to obtain an approximate value of Λ_{n+1}. The value of f_{n+1} is then found from Equation (35) which becomes

$$f_{n+1} = f_{f.p.}(1 + k_1 \Lambda_{(n+1)\,\mathrm{approx.}}). \tag{55}$$

f_{n+1} is then substituted back into (54) and a more accurate value of Λ_{n+1} is obtained. The change in the value of f corresponding to a given change in the value of Λ is small, and therefore only one iteration is generally necessary to obtain Λ with sufficient accuracy for the purposes of hand calculation.

If computations are to be performed by a high speed electronic computer it may be justifiable to use the value of Λ_{n+1} found by the above procedure to correct the values of H_{n+1} and f_{n+1} and perform successive integrations to find more accurate values of $[(\theta/L)\sqrt{R_L}]_{n+1}$, H_{n+1} and f_{n+1}. Using the iteration procedure in which mean values were substituted to find the new values, it was found that for both favourable and adverse pressure gradients the value of Λ converges to within 1 per cent after 2 cycles and to within $\frac{1}{2}$ per cent after 4 to 8 cycles.

The skin-friction parameter is given by Equation (45) which becomes, in non-dimensional form

$$c_f\sqrt{R_x} = \frac{2\tau_w}{\rho_a {u_a}^2}\sqrt{\frac{\rho_a u_a x}{\mu_a}} = \frac{\frac{\mu_1}{\mu_a}(12+\Lambda)\frac{u_1}{u_a}\left(\frac{x}{L}\right)^{1/2}}{3f\frac{\theta}{L}\sqrt{R_L}} \tag{56}$$

or

$$c_f\sqrt{R_x} = \frac{\frac{u_1}{u_a}\left(12+\Lambda\right)\left(\frac{x}{L}\right)^{1/2}}{3\left\{\Lambda\Big/\frac{\rho_1}{\rho_a}\frac{u_1'L}{u_a}\frac{\mu_w}{\mu_a}\right\}^{1/2}}. \tag{57}$$

If $c_f\sqrt{R_x}$ is defined in terms of the local conditions, the expression for skin friction becomes

$$[c_f\sqrt{R_x}]_{\mathrm{local}} = \frac{2\tau_w}{\rho_1 {u_1}^2}\sqrt{\frac{\rho_1 u_1 x}{\mu_1}} = \frac{(12+\Lambda)(x/L)^{1/2}}{3f\frac{\theta}{L}\sqrt{R_L}}\left[\frac{\rho_a}{\rho_1}\frac{u_a}{u_1}\frac{\mu_1}{\mu_a}\right]^{1/2}. \tag{58}$$

The reference condition, suffix a, may be defined anywhere in the isentropic flow regime over the surface. Usually it will be found convenient to define the reference condition as that immediately aft of the leading-edge shock wave, if any, but for the case of flow starting from a stagnation point on a body with a detached bow shock wave, the reference conditions are conveniently taken as the stagnation conditions. The reference velocity is then also conveniently taken as $u_a = a_0$ where a_0 is the speed of sound evaluated at the stagnation temperature.

The calculation procedure for the 'complete' method may now be summarized as follows:

(1) Find the values of H and f at $x/L = 0$ from Equations (40), (26) and (35). In most cases $\Lambda_{x=0} = 0$, but if this is not the case, then this parameter must be calculated from a known value of $\theta_{x=0}$ by an iterative process through Equations (54) and (35).

(2) From Equation (50) find $g_{x=0}$.

(3) Solve Equation (53) for $(\theta/L)\sqrt{R_L}$ at the point x_1/L.

(4) By Equation (54), using the value of $f_{x=0}$, find an approximate value of Λ_{x_1}.

(5) By Equations (26) and (35) find f_{x_1} using the appropriate value of k_1 from Figure 3 and the approximate value of Λ_{x_1}.

(6) A more accurate value of Λ_{x_1} may now be found from Equation (54).

(7) If a high speed computer is to be programmed for the problem, the new value of Λ_{x_1} may be fed in to the expressions for H, f and hence g and a new value of $(\theta/L)\sqrt{R_L}$ found from Equation (53). This procedure, (3) $\rightarrow$ (7), may be repeated until the value of Λ converges to a given tolerance. It may be found that the value of Λ will converge more rapidly if mean values are used in the iteration. In the examples considered, it has been found that Λ converges to within $\frac{1}{2}$ per cent of its previous value after 4 to 8 iterations.

For hand calculations, the refinement of the iterations through the momentum equation may be omitted with little additional error.

(8) From Equation (56) or (58) find $c_f\sqrt{R_x}$ or $[c_f\sqrt{R_x}]_{\text{local}}$.

(9) If step (7) has been omitted, the value of H_{x_1} may be found from Equation (40) using the value of Λ_{x_1} found in step (6) and the appropriate value of k_2 from Figure 5.

(10) Find g_{x_1} from Equation (50) and repeat the procedure to find the solution at x_2.

When evaluating the quadrature on the right hand side of Equation (53) a straight line function may be assumed if the range x_n to x_{n+1} is small.

However, if larger steps are taken, greater accuracy may be obtained by calculating values of the function at $x = x_{n-1}$ and $x = x_{n+2}$ using the values f_n and g_n. The actual shape of the function between x_n and x_{n+1} is then more accurately defined.

The size of the integration steps does not appear to be critical and, for hand calculations, steps over which the Mach number changes by 0·3 to 0·5 were found to be suitable. For automatic computation, smaller steps will give greater accuracy where the values of $|\Lambda|$ are small, but slight overcorrection may occur if separation is approached due to the errors involved at large values of $|\Lambda|$ in the assumption of linear correction factors for f and H.

For flows with favourable pressure gradients, the pressure gradient correction factors in the expressions for f and H are relatively small and this suggests that a slight simplification may be made to the computation procedure with little loss of accuracy in these cases. The simplification consists of dividing the flow regime into large sections over which the Mach number changes by about 1·0, and employing the values of $f_{f.p.}$, $H_{f.p.}$, and $g_{f.p.}$ found at the start of each section in the solution of the momentum equation over that section. Step-by-step correction of f and H is then omitted. For many cases of practical interest the calculation may be performed in one step and the method then is very similar to the 'first simple' method. This simplified procedure is now summarized and will be termed the 'Second simple' method.

5. *The 'Second Simple' Method—Computation Procedure.* (1) If the range of the Mach number of the flow over the surface is large, divide the problem into sections over which the change in Mach number is of the order of 0·5 to 1·0.

(2) Calculate $H_{f.p.}$ and $f_{f.p.}$, and hence $g_{f.p.}$, for each section from Equations (37), (26) and (50), taking values at the beginning of each section. These parameters are then assumed to be constant over the particular section.

(3) Evaluate the integral on the right hand side of Equation (53), numerically or graphically, and hence obtain

$$\left[\left(\frac{\rho_1}{\rho_a}\right)^2 \left(\frac{\theta}{L}\right)^2 R_L\right]_{n+1} - \left[\left(\frac{\rho_1}{\rho_a}\right)^2 \left(\frac{\theta}{L}\right)^2 R_L\right]_n \frac{[(u_1/u_a)^{g_n}]_n}{[(u_1/u_a)^{g_n}]_{n+1}}.$$

In most cases, such as the flow over a wing section with a sharp leading edge, the calculation may be performed in one step and then $(\theta/L)_n = 0$ which considerably simplifies the above expression.

(4) The value of $(\theta/L)\sqrt{R_L}$ may now be found.

(5) From Equation (54) calculate Λ.

(6) By substitution in Equation (56) or (58) find $c_f\sqrt{R_x}$ or $[c_f\sqrt{R_x}]_{\text{local}}$.

(7) Calculate the values of H *at each point* from Equation (40) using the appropriate value of k_2 from Figure 5. If the cooling rate is large and the value of Λ is large (>4), it may be necessary to use Figure 2 with a reasonable extrapolation to give the correction for H.

(8) The displacement thickness may now be calculated from the values of H and θ, and a second order correction for the effect of the displacement thickness on the pressure distribution made if required.

6. *Application of the Methods.* In order to illustrate the methods in use and to assess their accuracy for various types of flows, they have been applied to a range of cases involving both favourable and adverse pressure gradients, and have been compared with exact and other approximate solutions for some of these cases. In the following, the 'complete' method refers to the 'complete' method with step 7 of the procedure for that method omitted, unless otherwise stated. Further, these examples illustrate in general terms the effects of heat transfer on skin friction.

6.1. *Flows with Favourable Pressure Gradients.* In the following, capital letters are used to denote quantities in incompressible flow, and small letters to denote quantities in compressible flow.

Cohen and Reshotko[6] have presented the compressible flow solutions obtained by applying the Stewartson transformation[11] to a number of the similar solutions for incompressible flow presented by Falkner and Skan[7], and Hartree[12], corresponding to the free stream velocity distributions of the form

$$U_1 = CX^m. \qquad (59)$$

Here U_1 is the local incompressible flow free stream velocity,

X is the distance from a datum point,

and m is an exponent, constant for a particular flow, which can be of either sign.

With m positive, the incompressible flow corresponds to the flow along the face of a wedge, X being the distance from the stagnation point at the wedge apex.

In the example considered here, the flow has been assumed to accelerate from $M_1 = 0$ at the stagnation point where $x = X = X_1 = 0$, to $M_1 = 5 \cdot 0$ corresponding to $X = X_2 = L$, say. A high rate of heat transfer from the fluid to the surface of the body has been considered with $S_w = -0 \cdot 8$, that is, $T_w/T_r = 0 \cdot 2$,

where T_w is the wall temperature

and T_r is the recovery temperature.

The value of m has been taken as $\frac{1}{3}$.

It then follows readily from the Stewartson transformation that

$$\frac{x}{L} = \int_{X_1/L}^{X/L} \left[1 + 0 \cdot 2M_1^2\right]^4 d\left(\frac{X}{L}\right), \text{ for } \gamma = 1 \cdot 4. \tag{60}$$

When $X = X_2 = L$, Equation (60) yields the value of x/L at which $M_1 = 5 \cdot 0$.

Also

$$M_1 = 5 \cdot 0 \left(\frac{X}{L}\right)^{1/3}. \tag{61}$$

The solution for this case was evaluated from the results presented by Cohen and Reshotko[6] and the values of $(\theta/L)\sqrt{R_L}$, H, and $c_f\sqrt{R_x}$ were obtained, where

$$c_f = \frac{2\tau_w}{\rho_0 a_0^2}, \qquad R_L = \frac{\rho_0 a_0 L}{\mu_0}, \qquad R_x = \frac{\rho_0 a_0 x}{\mu_0}. \tag{62}$$

The 'complete' and the 'second simple' methods were then applied to this problem.

First, the 'complete' method was applied. The integration steps taken were those steps over which the free stream Mach number changed by $0 \cdot 5$, i.e., $M_1 = 0 \rightarrow M_1 = 0 \cdot 5$, $M_1 = 0 \cdot 5 \rightarrow M_1 = 1 \cdot 0$, . . . $M_1 = 4 \cdot 5 \rightarrow M_1 = 5 \cdot 0$. The results obtained are compared with the results of the exact solution in Figures 6 and 7 and are seen to be very accurate.

Secondly, the 'second simple' method was applied. In the 'second simple' method, the step-by-step corrections on f and H are omitted for the purposes of calculating θ and c_f. The flow was divided into large successive steps over which f and H, and hence g, were assumed constant and equal to the flat plate values appropriate to the beginning of the step. The steps selected, governed by the Mach number, were:

$$M_1 = 0 \rightarrow M_1 = 1 \cdot 0, \qquad M_1 = 1 \cdot 0 \rightarrow M_1 = 2 \cdot 0,$$
$$M_1 = 2 \cdot 0 \rightarrow M_1 = 3 \cdot 0, \qquad M_1 = 3 \cdot 0 \rightarrow M_1 = 5 \cdot 0.$$

The simplification of ignoring the effects of pressure gradient on f and H for the purposes of calculating θ and c_f reduces the complexity of the calculations and hence reduces the computation time. This may be of importance for calculations performed on a hand machine but is of little consequence if a high speed computer is employed. The values of c_f and θ obtained by the 'second simple' method, also shown in Figures 6 and 7, were hardly less accurate than those obtained by the 'complete' method. To determine H more accurately, however, the pressure gradient correction of Equation (40) was applied using the values of Λ already found from the shortened method which ignored this correction. Again, it may be seen from Figures 6 and 7, the results were almost as good as those obtained by the 'complete' method. The need to obtain H accurately stems from the need to obtain the displacement thickness δ^* for second order calculations allowing for the influence of the boundary layer on the external flow[8, 13].

The second example to be considered involving a favourable pressure gradient is the case of a Mach number distribution which increases linearly along the surface from an initial value of 4·0 at $x/L = 0$ to a value of 8·0 at $x/L = 1·0$.
That is

$$M_1 = M_a\left(1 + \frac{x}{L}\right), \qquad M_a = 4·0.$$

The calculation was performed using

(*a*) the 'complete' method, with $\omega = \sigma = 1$ and also with $\omega = 0·89$ and $\sigma = 0·725$

(*b*) the 'first simple' method in which the values of f, H, and hence g are assumed constant throughout and equal to the flat plate value at $x/L = 0$

and (*c*) the 'second simple' method with one step only, $M_1 = 4 \rightarrow M_1 = 8$.
In all cases results were evaluated for cooling such that the wall temperature T_w equalled the reference temperature T_a in the free stream at $x/L = 0$. The results of these calculations are presented in Figures 8 and 9.

To illustrate the effect of heating the wall, the 'complete' method was used to evaluate the above case for a heated wall with $S_w = +0·4$, that is $T_w = 1·4\ T_r$, for $\omega = 0·89$ and $\sigma = 0·725$.

It was found in the solution of the highly cooled wall case by the 'complete' method that the assumption of constant linear correction factors for f and H caused severe overcorrection of these parameters as the value of Λ increased, with consequent discontinuities in the slopes of the θ and c_f distribution curves. However, use of the direct relationship between f and Λ, Figure 2, resulted in more acceptable results being obtained. It should be noted that this case represents an extremely strong favourable pressure gradient unlikely to be approached in practice.

The magnitude of the error incurred by the omission of step 7 of the procedure for the 'complete' method may be gauged by reference to Figure 8. Here the 'complete' method with iterations through the solution of the momentum equation repeated until Λ was within $\frac{1}{2}$ per cent of its previous value, is compared with the 'complete' method with step 7 omitted, for the linear Mach number distribution case. Again it should be noted that this may be regarded as a severe test.

6.2. *Flows with Adverse Pressure Gradients.* Curle[3] has referred to two 'exact' solutions for retarded flows obtained by the Mathematics Division of the National Physical Laboratory by simultaneous integration of the momentum and energy equations. These solutions have been assessed as being within $\pm$ 5 per cent of the true solution, but it is reasonable to suppose that they are more accurate over the first part of the solution than towards the separation point. The solutions were for a linearly retarded velocity distribution with an initial Mach number of 4·0, $\omega = \sigma = 1$, and $T_w = T_a$: and for a linearly increasing pressure distribution with initial Mach number of 2·0, $\omega = \sigma = 1$, and $T_w = T_a$. That is,

$$u_1 = u_a\left(1 - \frac{x}{L}\right), \quad M_a = 4·0, \quad T_w = T_a, \quad \omega = \sigma = 1 \tag{63}$$

and

$$p_1 = p_a\left(1 + \frac{x}{L}\right), \quad M_a = 2·0, \quad T_w = T_a, \quad \omega = \sigma = 1. \tag{64}$$

These solutions have been used to assess the accuracy of the present methods, and of other approximate methods, for cases involving adverse pressure gradients.

It will be noted that the solutions obtained by the N.P.L. have been termed 'exact', the inverted commas indicating that doubts have been cast on the accuracy of these solutions. In order to check further the accuracy of the present methods for adverse pressure gradients, a 'similar' solution from the set obtained by Cohen and Reshotko[6] has been used.

To make use of a 'similar' solution of the form $U_1 = CX^m$ for an adverse pressure gradient ($m < 0$), it is necessary to start with a non-zero value of X to avoid an infinite velocity at the origin. The assumption made in the example considered here was that $x/L = 0$ when $X/L = 0 \cdot 001$. The power law distribution was prescribed to give a decrease in Mach number from $4 \cdot 001$ to $1 \cdot 625$ over the range $X/L = 0 \cdot 001$ to $X/L = 1 \cdot 0$, with $\beta = 2m/(m+1) = -0 \cdot 3$ (that is, $m = -0 \cdot 13043$), and $S_w = -0 \cdot 8$.
We then find that

$$M_1 = 1 \cdot 625 \left(\frac{X}{L}\right)^{-0 \cdot 13043} \tag{65}$$

and

$$\frac{x}{L} = \int_{0 \cdot 001}^{X/L} \left[1 + 0 \cdot 5281 \left(\frac{X}{L}\right)^{-0 \cdot 26086} \right]^4 d\left(\frac{X}{L}\right) \tag{66}$$

for $\gamma = 1 \cdot 4$.

The values of θ, H and c_{f0} were obtained for this distribution from the values of the transformed momentum thickness $\theta_{tr.}$, form factor $H_{tr.}$, and wall shear function f_w'', tabulated by Cohen and Reshotko[6].

The momentum thickness has a finite value at $x/L = 0$, and the value of $(\theta/L)\sqrt{R_{L_0}}$ given by the exact 'similar' solution was used as a starting value at $x/L = 0$ for the 'complete' method. An iterative process through Equations (54) and (35), leading to constant values of Λ and f, was used at $x/L = 0$. Following this the method proceeded normally. The values of θ, H, and c_f found from the 'complete' method with steps of integration governed by given changes in the free stream Mach number, are compared with the results from the 'similar' solution in Figure 14. It should be noted that this case also provides a severe test of the method since it concerns a boundary layer which, at the chosen origin, was of finite thickness and which had previously been subjected to an adverse pressure gradient increasing in intensity to infinity as $X = 0$ was approached. Consequently the magnitude of Λ was already large (-3) at the origin and the corrections due to it were correspondingly important. The success of the method in this particular case lends support, therefore, to the inference that it can handle a wide range of cases involving rapidly varying external pressure distributions.

7. *Comparison of the Methods.* An exact solution involving a favourable pressure gradient with which to compare the approximate methods is the 'similar' solution for the flow accelerating from $M_1 = 0$ to $M_1 = 5 \cdot 0$ derived from the set presented by Cohen and Reshotko[6]. The 'complete' and the 'second simple' methods, Figures 6 and 7, both give results which are remarkably accurate. Figure 7 has been plotted on a logarithmic scale to allow the results near to the stagnation point to be presented in detail. On the basis of this comparison it may be concluded that the 'complete' method and the 'second simple' method with suitably chosen calculation steps both yield results of acceptable accuracy for flows involving favourable pressure gradients.

On the basis of the comparison between the 'complete' method and the 'complete' method with step 7 for the case $M_1 = M_a(1+x/L)$, it may be concluded that the iteration through the momentum equation has only a small effect on the final values of skin-friction coefficient obtained, and may therefore be omitted in most instances.

The results given by the 'first simple' method for the linear Mach number distribution, Figure 8, indicate that it somewhat overestimates the values of θ and c_f for a strong favourable pressure gradient.

From Figure 8 may be gauged the effect of taking a step over which the change in Mach number is large in the application of the 'second simple' method. It may be seen that the error, using the 'complete' method as the standard, is relatively small. This error would certainly have been reduced had the calculation been divided into two or four steps. As the computation effort involved in the 'second simple' method is less than that in the 'complete' method, and the results obtained in the two favourable pressure gradient examples considered are not materially different for the two methods, the 'second simple' method may be generally recommended for this class of problem.

It will be recalled that the definition of Λ for the 'first simple' method, Equation (4), is different from that for the 'complete' and 'second simple' methods, Equation (44), due to the different transformations of the y co-ordinate employed. However, the form of the final expressions for skin friction for all the methods is the same, Equations (24) and (57). For a favourable pressure gradient ($\Lambda > 0$), the skin friction is relatively insensitive to the value of Λ, but for an adverse pressure gradient ($\Lambda < 0$), an increase in Λ reduces the factor $(12+\Lambda)$ and increases the denominator of the expression. Hence the value of the skin-friction coefficient is very sensitive to the value of Λ with an adverse pressure gradient. As the expressions for Λ are dependent on f, it may be expected that the omission of the pressure gradient term in the calculation of f will yield unsatisfactory results for the skin-friction coefficient when the pressure gradient is strongly adverse. This effect is illustrated by the results for the N.P.L. case involving adverse pressure gradients. From Figure 10, it may be seen that while the 'complete' method yields reliable results the 'second simple' method overestimates the skin friction and the 'first simple' method underestimates the skin friction. The conclusion may be drawn, therefore, that for cases involving large adverse pressure gradients the 'complete' method must be used if reliable results are to be obtained.

Figure 10 illustrates the effects of inclusion or exclusion of step 7 of the 'complete' method and of varying the length of the integration steps when the pressure gradient is adverse. The iteration through the solution of the momentum equation improves the accuracy over the first part of the calculation, but the errors involved in the assumption of linear correction factors become amplified as separation is approached. When step 7 is excluded, a slightly better agreement is obtained near separation but the accuracy in this region is still not very high. Direct use of Figures 2 and 4 instead of linear factors to correct f and H would lead to a better prediction of separation. The use of uneven increments during the calculation procedure does not introduce significant additional errors.

8. *Comparison with Other Approximate Methods.* The approximate methods presented by Cohen and Reshotko[6] and Curle[3] were used to calculate the N.P.L. adverse gradient cases referred to previously. Both these methods follow similar lines to the Thwaites[9] method for incompressible

flow, but where Cohen and Reshotko used their set of transformed 'similar' solutions as the basis for universal parametric relationships, Curle used the Thwaites incompressible flow parameters, as modified by Curle and Skan[14], and employed the assumption of a quadratic relationship between the temperature and the velocity boundary-layer profiles. Both these methods require that $\omega = \sigma = 1$. The Cohen and Reshotko method was applied to the 'similar' solution case for the flow starting from a stagnation point and accelerating to $M_1 = 5$. It is to be expected that the Cohen and Reshotko method will give accurate results for this case as it represents one of the 'similar' solutions on which the method is based. It should be noted, however, that on the whole the results given by the Cohen and Reshotko method, Figures 6 and 7, are not quite as close to the 'similar' solution as are the results given by the 'complete' method of this paper, although the differences are small. A possible error can arise from the choice of the constant B in Equation (31) of Cohen and Reshotko's paper. This equation is

$N = A + Bn$ where N is the momentum parameter

and n is the correlation parameter.

The constant A is well defined, being $0 \cdot 44$, but the value of B is dependent on the choice of the best straight line approximation to the $N \sim n$ relationship.

The 'complete' method of this paper is compared in Figure 11 with the Cohen and Reshotko method and with the Curle method for the linearly retarded velocity distribution calculated by the N.P.L. From the results in Figure 11 it may be seen that, on the whole, the 'complete' method gives the most accurate results.

It may be argued that conditions approaching separation in supersonic flow are not of major practical interest as, for most practical cases, pressure gradients are favourable. Small regions of adverse pressure gradient may possibly occur due to the interaction of a shock wave with the boundary layer, or unusual surface curvature, but these effects are likely to be accompanied by transition and will seldom produce a simple laminar boundary-layer separation. If we accept a realistic upper limit for the supersonic compression which may occur as being the compression equivalent to a change of about 10 deg in the flow direction in a simple wave flow, we can estimate the range of practical interest for the linearly retarded velocity distribution case of Figure 11, and the linearly increasing pressure distribution of Figure 13. This indicates a practical range of x/L from $x/L = 0$ to $x/L = 0 \cdot 05$ for the linearly retarded velocity distribution, and from $x/L = 0$ to $x/L = 0 \cdot 70$ for the linearly increasing pressure distribution. On this basis there is little to choose between the 'complete' method and the Cohen and Reshotko method for the linearly retarded velocity distribution, and Curle's method yields results which are high. However, in the less severe case of the linearly increasing pressure distribution, the 'complete' method yields materially closer results to the 'exact' solution than the other two methods.

From this comparison it is fair to conclude that the present 'complete' method is applicable with a higher degree of accuracy to a wider range of cases than the other approximate methods examined. Its main advantages over the other methods are:

1. It is not restricted to values of the Prandtl number and of the temperature-viscosity relationship index of unity, but is applicable to all cases where they are near unity.
2. It predicts not only the skin-friction distribution accurately but similarly predicts the distributions of the momentum and displacement thicknesses.

3. In principle the 'complete' method may be used for cases involving non-uniform surface temperature, although its accuracy in this application has not been tested.

4. The method may be programmed readily for solution of problems on a high speed computer.

9. *Physical Interpretation of some of the Results obtained.* 9.1. *Effects of Heat Transfer and Pressure Gradient on Skin Friction.* Consideration of Figure 12 indicates that cooling of the surface, when the pressure gradient is adverse, increases the skin friction. However, in the case illustrated in Figure 9, where the pressure gradient is favourable, cooling decreases the skin friction. The reverse is true in each case when the wall is heated. In the case of the adverse pressure gradient the increase in skin friction with cooling is associated with a marked increase in the distance to separation, a result previously noted by Gadd[15], Morduchow and Grape[1] and others.

It appears that the most important effect of wall temperature on the skin friction in the presence of a pressure gradient is through its effect on the parameter Λ and hence on the factor $(12+\Lambda)$ in the expression for c_f in Equation (56). Thus from Equation (54) we see that raising the wall temperature, for example, increases μ_w and therefore increases $|\Lambda|$. Related changes are also produced in $f\theta$ but these are smaller in their effects on Λ and c_f. With an adverse pressure gradient Λ is negative and hence heating of the wall reduces the factor $(12+\Lambda)$ and so reduces the skin friction. With a favourable pressure gradient on the other hand Λ is positive and so the factor $(12+\Lambda)$ is increased and with it is increased the skin friction. Converse effects occur with wall cooling.

In so far as the effects of heat transfer and pressure gradient on the skin friction may be related to the associated effects on Λ they can be linked with their effects on the form of the velocity profile near the wall. Illingworth[16] has suggested a more direct physical interpretation by considering the change in the response of the fluid close to the wall with change of wall temperature to the external pressure gradient. Thus, with wall heating the fluid density close to the wall is reduced and so the fluid is more readily decelerated by an adverse pressure gradient and more readily accelerated by a favourable pressure gradient. Thus, in the former case the skin friction is reduced and flow separation occurs earlier, whilst in the latter case the skin friction is increased.

9.2. *Effects of Changes of ω and σ.* In the case of a flat plate at zero incidence it has been shown[5] that the effect of heat transfer on the skin friction is determined by the value of $(1-\omega)$. If $\omega < 1$, cooling increases the skin friction, and if $\omega > 1$, cooling decreases the skin friction at a given Mach number but the effects are small for small values of $(1-\omega)$. To illustrate the overall effect of ω and σ on the skin friction in the presence of pressure gradient and heat transfer, two cases were calculated with $\omega = 0{\cdot}89$ and $\sigma = 0{\cdot}725$. The favourable pressure gradient case is shown in Figure 9 and it may be seen that where there is cooling such that $T_w = T_a$, the difference between the skin friction for the above values of ω and σ and that for $\omega = \sigma = 1$ is very small. However, when there is zero heat transfer, a difference results of the order of 10 per cent in the skin friction. A similar result is shown for the adverse gradient case in Figure 12, but then the change in skin friction with zero heat transfer is of opposite sign to that with the pressure gradient favourable.

These results are not by themselves enough to enable us to disentangle the separate effects of the changes in ω and σ on the skin friction, but we can note that in general they are likely to be small for values of these parameters of practical interest. However, it is hardly surprising that when the wall temperature (T_w) is kept the same as the reference temperature (T_a) the resulting changes in skin friction are negligible, since the important flow conditions close to the wall are then hardly affected by the changes in ω and σ. For the case of zero heat transfer the dominant effect is probably that of the change of σ, since with $S_w = 0$ the wall temperature T_w must be reduced with reduction of σ. This would result as already explained in a reduction of the skin friction with the pressure gradient favourable and an increase of skin friction with the pressure gradient adverse in conformity with the results illustrated in Figures 9 and 12. The associated effects of the change in ω for the case of zero heat transfer or constant S_w are difficult to assess in general terms since they depend on the relative magnitudes of T_1, T_w and T_a as well as on the pressure gradients but they are probably smaller than the effects due to the change in σ.

10. *Conclusions.* Three methods have been presented for the calculation of the skin friction and other parameters in the laminar compressible boundary layer with heat transfer and non-uniform free-stream pressure distribution.

The methods are applicable to flows with both adverse and favourable pressure gradients, and they have been compared with exact solutions in four diverse cases. It has been shown that for flows involving adverse pressure gradients the 'complete' method gives the most reliable results. The 'complete' and 'second simple' methods are applicable to the type of flow found on a wing having a rounded leading edge. The 'first simple' method yields reasonable results in many practical cases involving small favourable pressure gradients, as do both the 'complete' and 'second simple' methods.

All three methods are general for values of ω and σ near, but not necessarily equal to, unity.

In the 'complete' method the effect of pressure gradient on the various boundary-layer parameters has been taken into account by employing simple correction factors derived from the 'similar' solutions of Cohen and Reshotko[6]. This permits accurate values of the momentum thickness (θ) and of the form factor (H), as well as of the skin-friction coefficient (c_f), to be obtained.

The 'complete' method may be used to calculate cases involving non-uniform surface temperature, but the accuracy of the method under these conditions has not been investigated.

The general effects of heat transfer on the skin friction in a laminar boundary layer have been illustrated by the examples considered. It has been shown that when the pressure gradient is favourable, cooling of the surface decreases the skin friction, and when the pressure gradient is adverse, cooling increases the skin friction. These effects have been explained physically in terms of the influence of heat transfer on the fluid properties close to the wall and the effect of heat transfer and pressure gradient on the velocity distribution in the boundary layer.

It has been shown that with values of ω and σ of $0 \cdot 89$ and $0 \cdot 725$, the skin friction is altered very little from the values found with $\omega = \sigma = 1$ when the wall is cooled to approximately the free stream temperature. Under zero heat transfer conditions the alteration is more marked, and its sign depends on the sign of the pressure gradient (Figures 9 and 12).

NOTATION

a		Velocity of sound
a, b, c, d		Constants in the modified Pohlhausen velocity distribution
c		Chord
c_p		Specific heat at constant pressure
c_f		Local skin-friction coefficient based on reference conditions
	$=$	$2\tau_w/\rho_a u_a^2$
c_{f0}		Local skin-friction coefficient based on stagnation conditions
	$=$	$2\tau_w/\rho_0 a_0^2$
f_w''		Wall shear function tabulated by Cohen and Reshotko[6]
$f_{f.p.}$		Function of M_1, T_w/T_1, ω and σ defined in Equation (26)
	$=$	Flat plate value of δ_1/θ
f		Corrected value of δ_1/θ, Equation (35)
g		Function defined in Equation (13), or Equation (50)
i		Ratio of enthalpies
	$=$	I/I_1
k		Coefficient of thermal conductivity
k_1		Correction factor in Equation (35)
k_2		Correction factor in Equation (40)
l, n, r		Correlation parameters used by Cohen and Reshotko[2]
p		pressure
r		Recovery factor
	$=$	$(T_r - T_1)/(T_0 - T_1)$
u		Velocity in the x direction
v		Velocity in the y direction
x		Distance measured along the surface
y		Distance measured normal to the surface
A, B		Constants in Equation (31) of Cohen and Reshotko[2]
C		Constant in power law velocity distribution
C_F		Overall skin-friction coefficient based on leading-edge conditions
H		Form factor
	$=$	δ^*/θ
$H_{tr.}$		Transformed form factor of Cohen and Reshotko[2]
I		Enthalpy
L		Reference length
M		Mach number

R		Reynolds number: suffices indicate values on which R is based
S		Temperature ratio parameter
	$=$	$T/T_r - 1$
T		Absolute temperature
U		Velocity in the X direction in incompressible flow
X		Distance along surface in incompressible flow
Y		Transformed distance normal to surface
γ		Ratio of specific heats
δ		Value of y defining outer edge of boundary layer
δ_1		Value of Y corresponding to $y = \delta$
δ^*		Displacement thickness
η	$=$	u/u_1, Equation (8)
θ		Momentum thickness
μ		Coefficient of viscosity
ν		Kinematic viscosity
	$=$	μ/ρ
ρ		Density
σ		Prandtl number
	$=$	$\mu c_p/k$
τ		Shear stress
ω		Temperature-viscosity relationship index
Λ		Pressure gradient parameter, Equations (4) and (44)

Suffices

a	Reference values in the free stream
∞	Reference values upstream of the leading-edge shockwave
0	Stagnation conditions
r	Recovery conditions
1	Values at outer edge of boundary layer
$i, 0$	Zero heat transfer in incompressible flow
$tr.$	Transformed values
w	Wall values
$n, n+1$, etc.	Values at x_n, x_{n+1}, etc.
local	Parameters defined by local conditions

Unless otherwise stated, an accent denotes differentiation with respect to x/L.

(82878) B*

REFERENCES

No.	Author	Title, etc.
1	M. Morduchow and R. G. Grape ..	Separation, stability and other properties of compressible laminar boundary layers with pressure gradient and heat transfer. N.A.C.A. Tech. Note 3296. May, 1955.
2	C. B. Cohen and E. Reshotko ..	The compressible laminar boundary layer with heat transfer and arbitrary pressure gradient. N.A.C.A. Report 1294. 1956.
3	N. Curle	The steady compressible laminar boundary layer, with arbitrary pressure gradient and uniform wall temperature. *Proc. Roy. Soc. A.* 249. pp. 206 to 224. 1958.
4	R. J. Monaghan	Effects of heat transfer on laminar boundary layer development under pressure gradients in compressible flow. A.R.C. R. & M. 3218. May, 1960.
5	A. D. Young	Skin friction in the laminar boundary layer in compressible flow. *Aero. Quart.* Vol. 1. pp. 137 to 164. August, 1949.
6	C. B. Cohen and E. Reshotko ..	Similar solutions for the compressible laminar boundary layer with heat transfer and arbitrary pressure gradient. N.A.C.A. Report 1293. 1956.
7	V. M. Falkner and S. W. Skan ..	Some approximate solutions of the boundary layer equations. A.R.C. R. & M. 1314. 1930.
8	A. D. Young	The calculation of the profile drag of aerofoils and bodies of revolution at supersonic speeds. College of Aeronautics Report No. 73. April, 1953.
9	B. Thwaites	Approximate calculation of the laminar boundary layer. *Aero. Quart.* Vol. 1. pp. 243 to 280. November, 1949.
10	N. Curle	The effects of heat transfer on laminar boundary layer separation in supersonic flow. A.R.C. 21,986. May, 1960.
11	K. Stewartson	Correlated incompressible and compressible boundary layers. *Proc. Roy. Soc. A.* Vol. 200. No. A.1060. pp. 84 to 100. December, 1949.
12	D. R. Hartree	On an equation occurring in Falkner and Skan's approximate treatment of the equations of the boundary layer. *Proc. Camb. Phil. Soc.* Vol. 33. Part 2. pp. 223 to 239. April, 1937.
13	A. D. Young and S. Kirkby	Effects of interaction between boundary layers and external stream and of incidence on boundary-layer drag at supersonic speeds. A.R.C. C.P. 451. November, 1958.

No.	Author	Title, etc.
14	N. Curle and S. W. Skan	Approximate methods for predicting separation properties of laminar boundary layers. *Aero. Quart.* Vol. VIII. pp. 257 to 268. August, 1957.
15	G. E. Gadd	The numerical integration of the laminar compressible boundary layer equations, with special reference to the position of separation when the wall is cooled. A.R.C. C.P. 312. August, 1952.
16	C. R. Illingworth	The effect of heat transfer on the separation of a compressible laminar boundary layer. *Quart. J. Mech. App. Math.* V. 7. Pt. I. pp. 8 to 34. 1954.

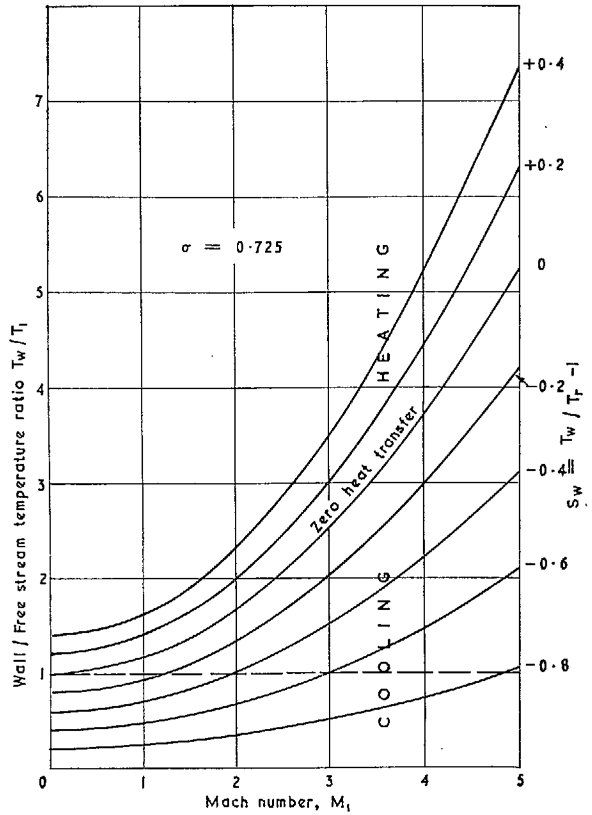

FIG. 1. Relationship between Mach number, S_w and T_w/T_1. $\sigma = 0{\cdot}725$.

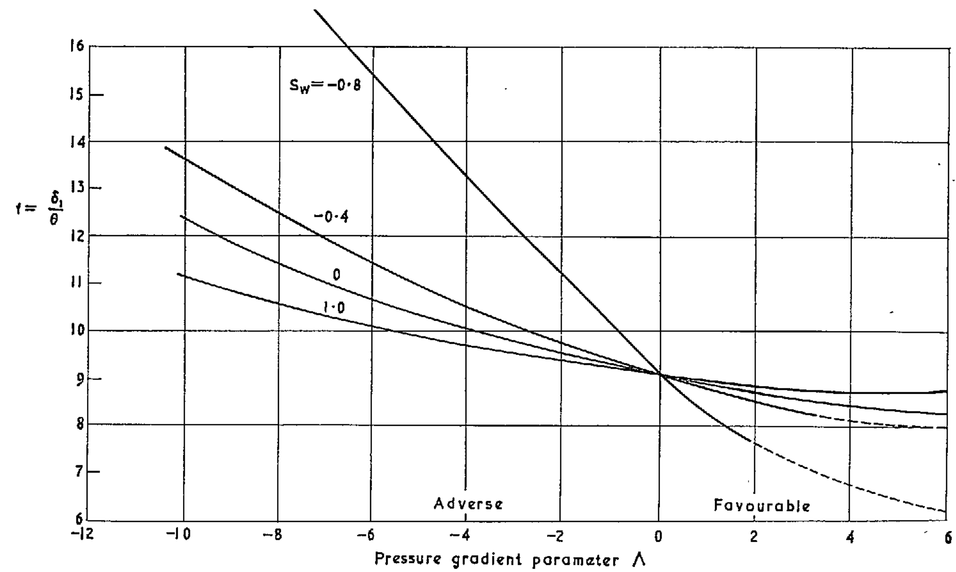

FIG. 2. Relationship between $f = \delta_1/\theta$ and Λ, derived from Cohen and Reshotko (Ref. 6).

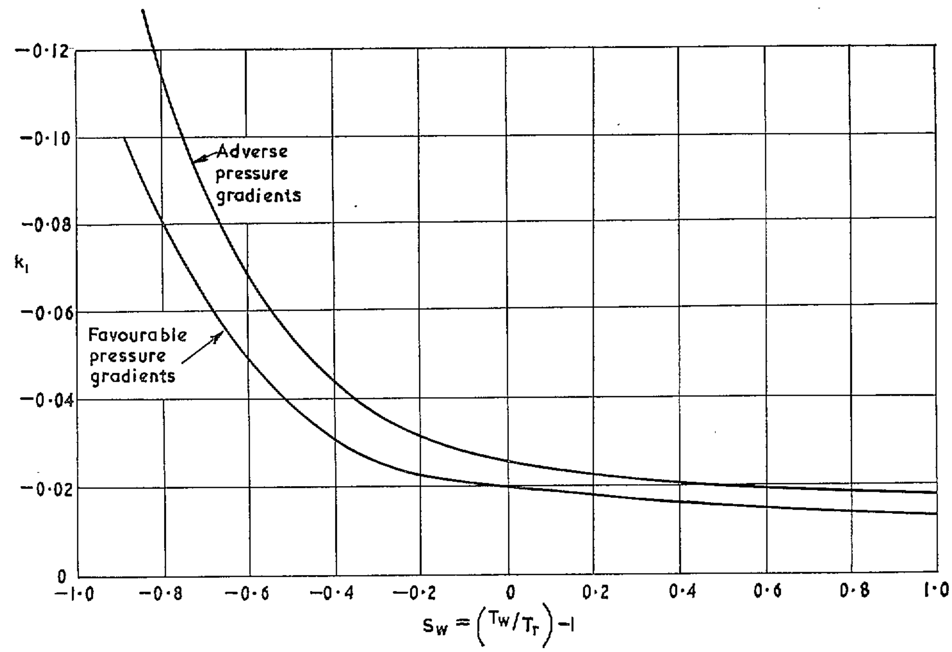

FIG. 3. Correction factor k_1 in Equation (35), $f = \delta_1/\theta = f_{f.p.}(1 + k_1\Lambda)$.

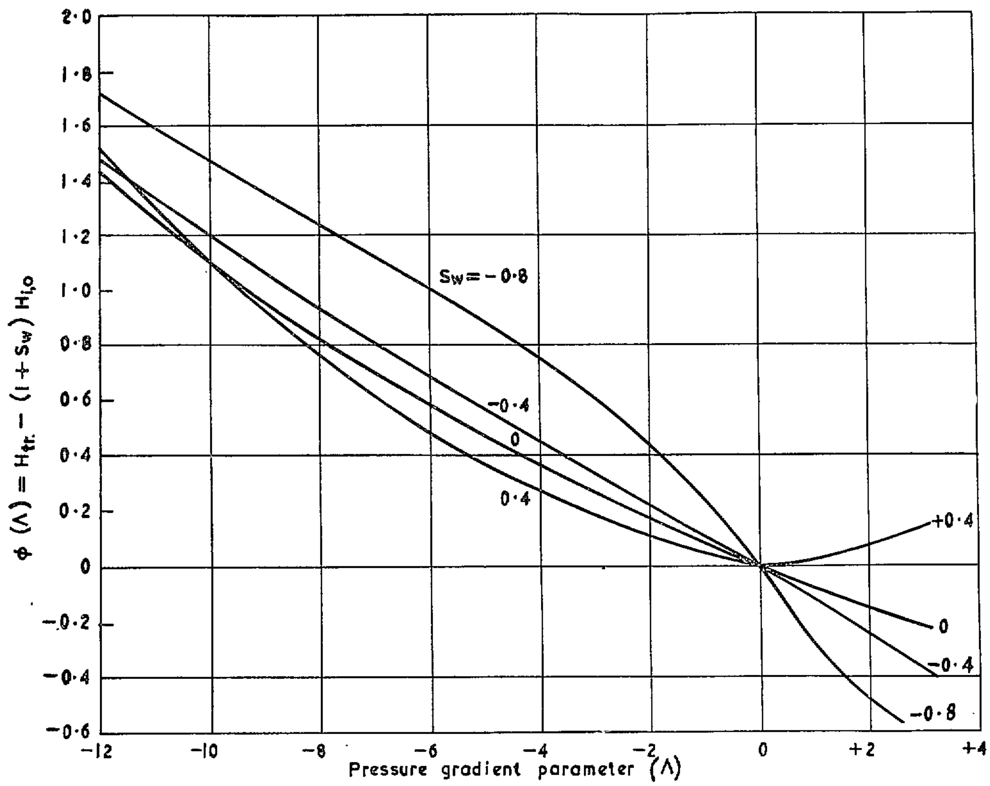

FIG. 4. Function $\phi(\Lambda)$, Equation (39), derived from Cohen and Reshotko (Ref. 6).

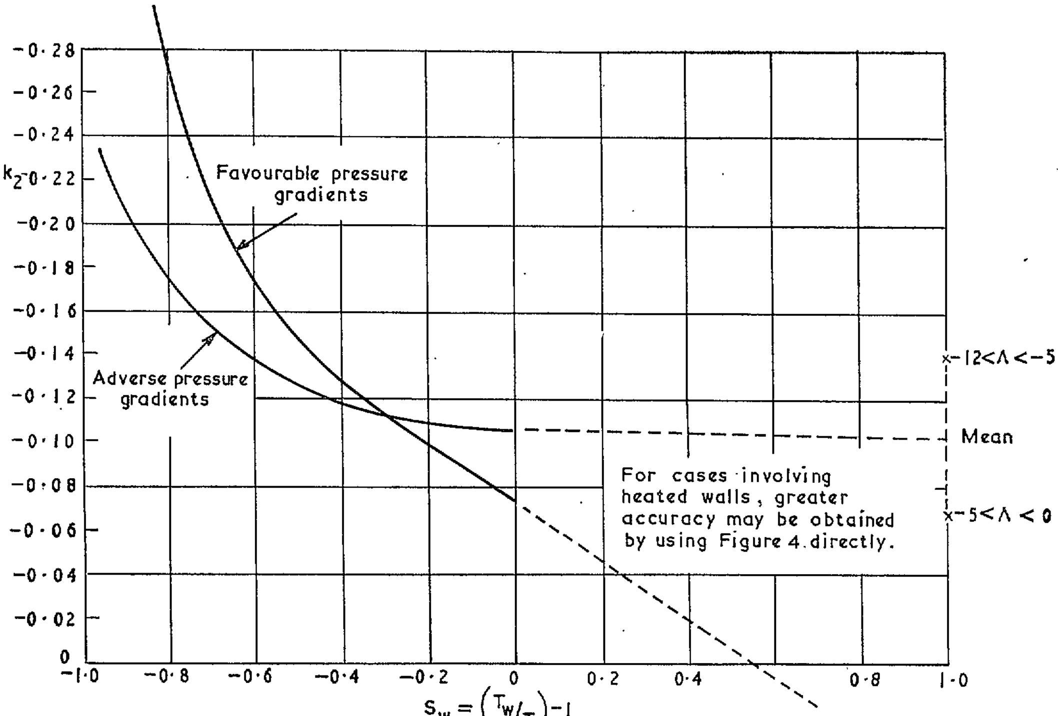

FIG. 5. Correction factor k_2 in Equation (40),

$$H = \left[(1+S_w)H_{i,0} + k_2\Lambda\right]\left(1 + \frac{\gamma-1}{2} M_1^2 \sigma^{1/2}\right) + \frac{\gamma-1}{2} M_1^2.$$

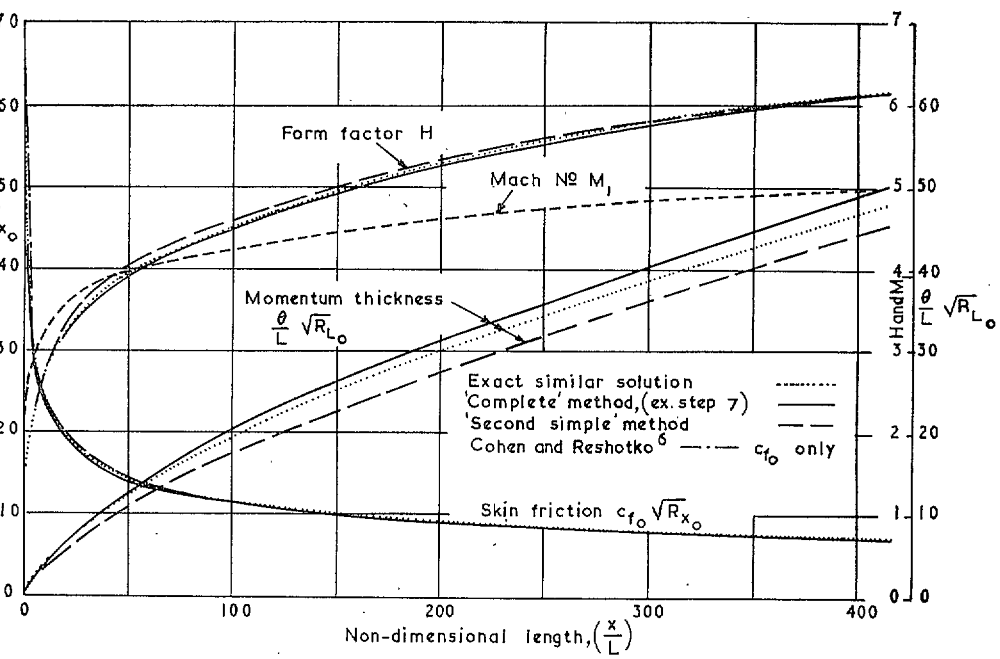

FIG. 6. Flow accelerating from stagnation point.

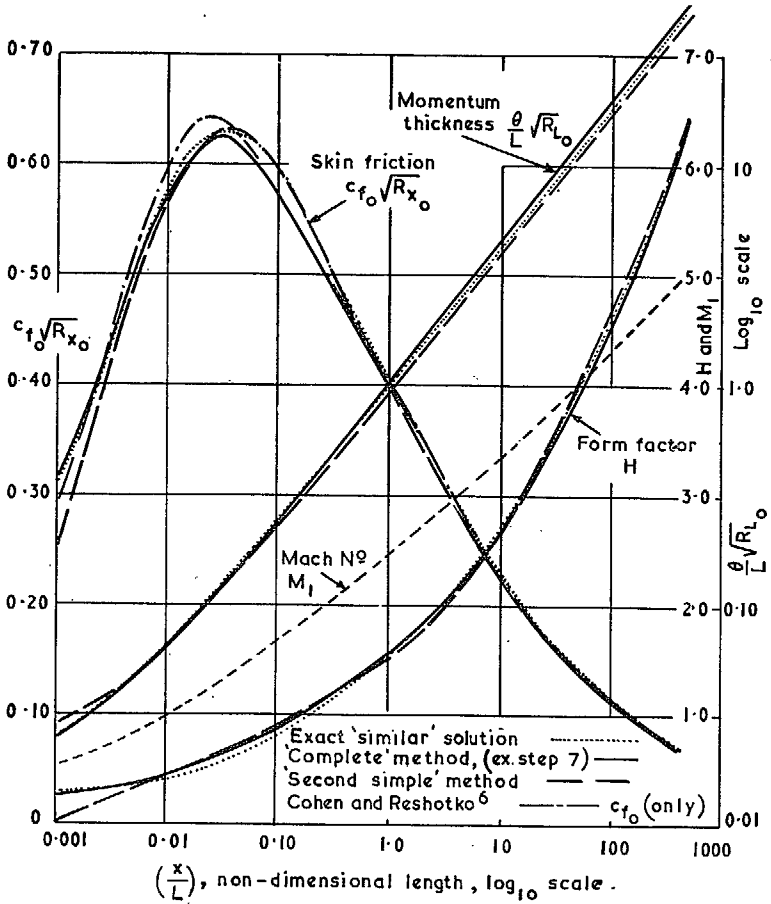

FIG. 7. Flow accelerating from stagnation point.

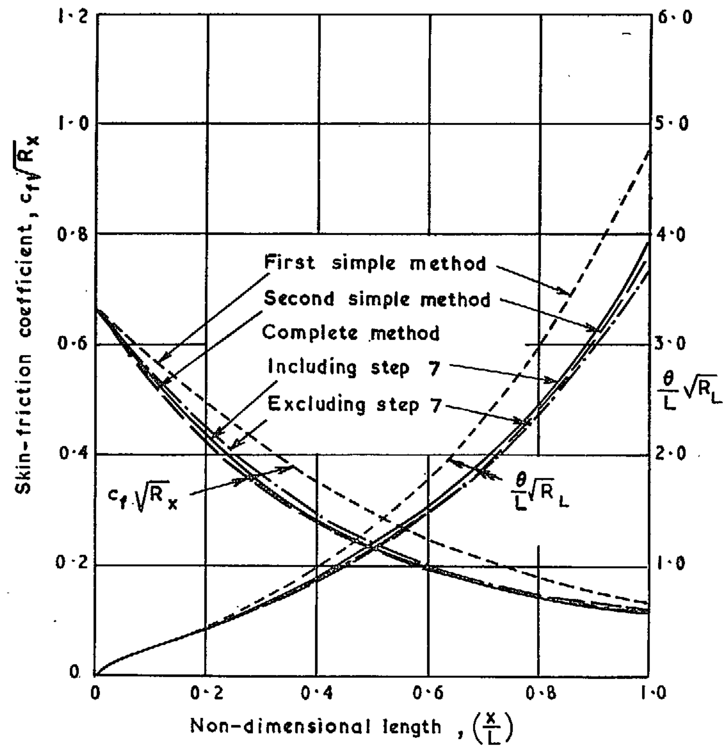

FIG. 8. Comparison of forms of method, large favourable gradient; $M_1 = M_a(1 + x/L)$, $M_a = 4\cdot0$, $\omega = \sigma = 1$, $S_w = -0\cdot762$.

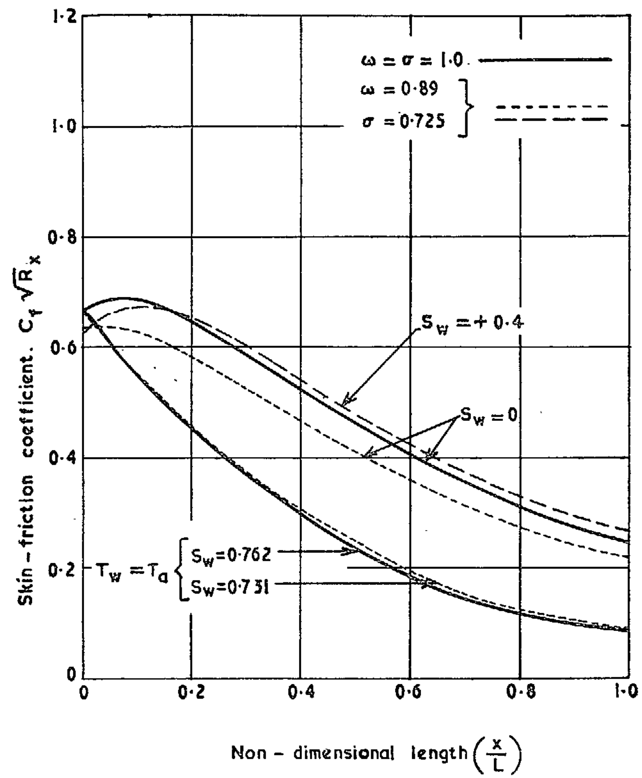

FIG. 9. Effect of wall temperature ratio and of ω and σ on skin friction, $x_T/L = 1 \cdot 0$, $M_1 = M_a\,(1 + x/L)$, $M_a = 4 \cdot 0$.

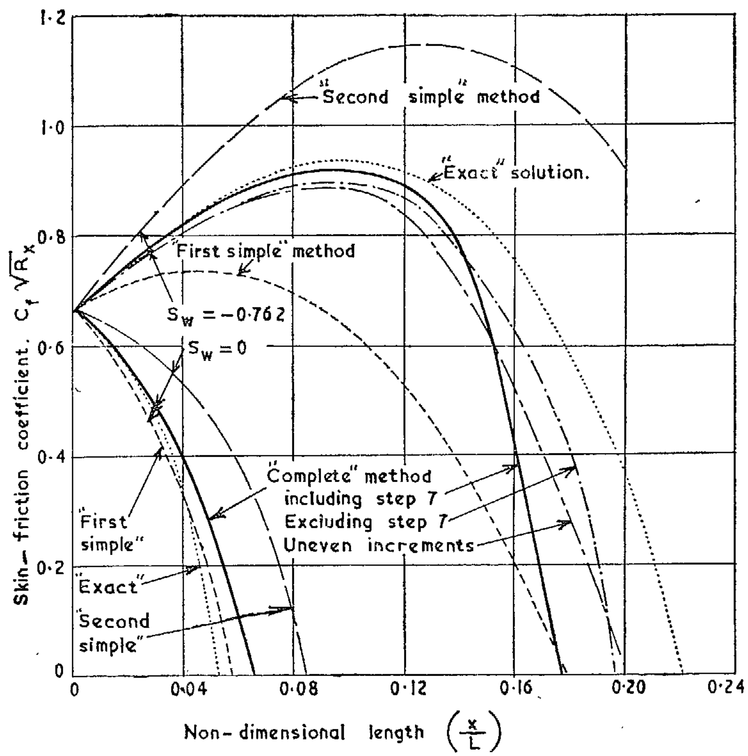

FIG. 10. Comparison of forms of method, large adverse gradient; $u_1 = u_a\,(1 - x/L)$, $M_a = 4 \cdot 0$, $\omega = \sigma = 1$, $S_w = -\,0 \cdot 762$ and $S_w = 0$.

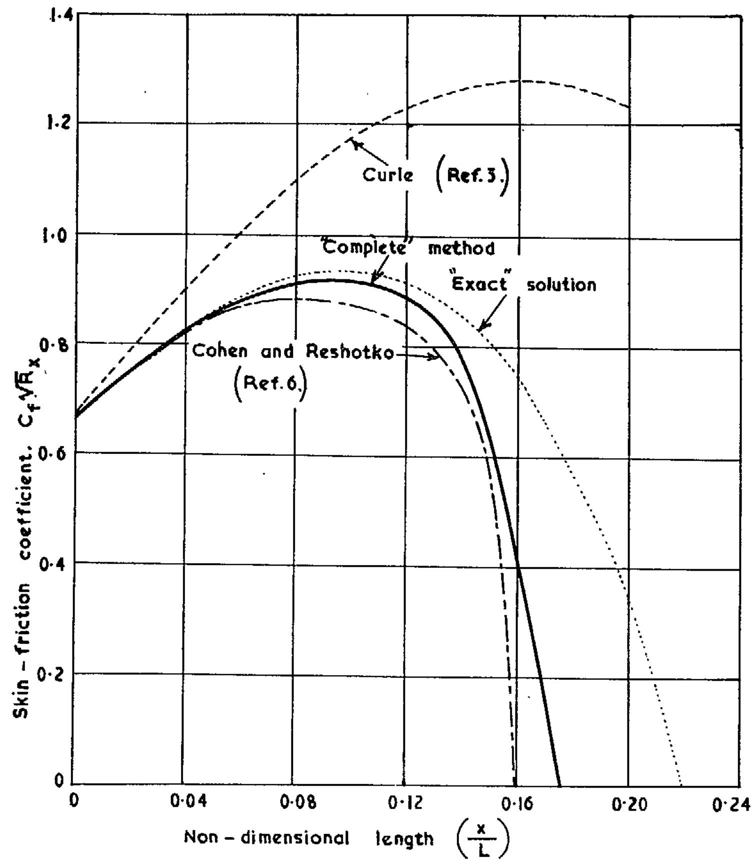

FIG. 11. Comparison of approximate methods, adverse gradient case; $u_1 = u_a(1 - x/L)$, $M_a = 4 \cdot 0$, $\omega = \sigma = 1$, $S_w = -0 \cdot 762$, $(T_w = T_a)$.

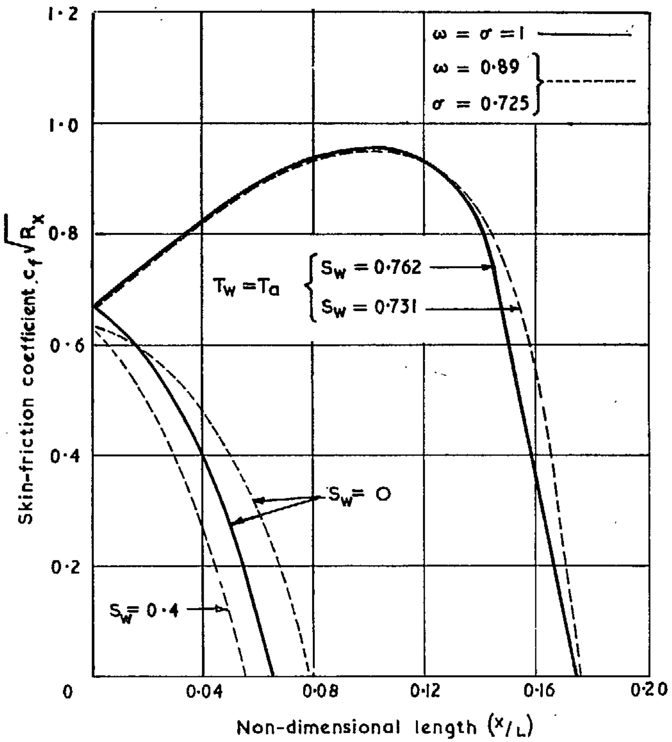

FIG. 12. Effect of wall temperature ratio and of ω and σ on skin friction, $u_1 = u_a(1 - x/L)$, $M_a = 4 \cdot 0$, $(x_T/L) > (x_{sep}/L)$.

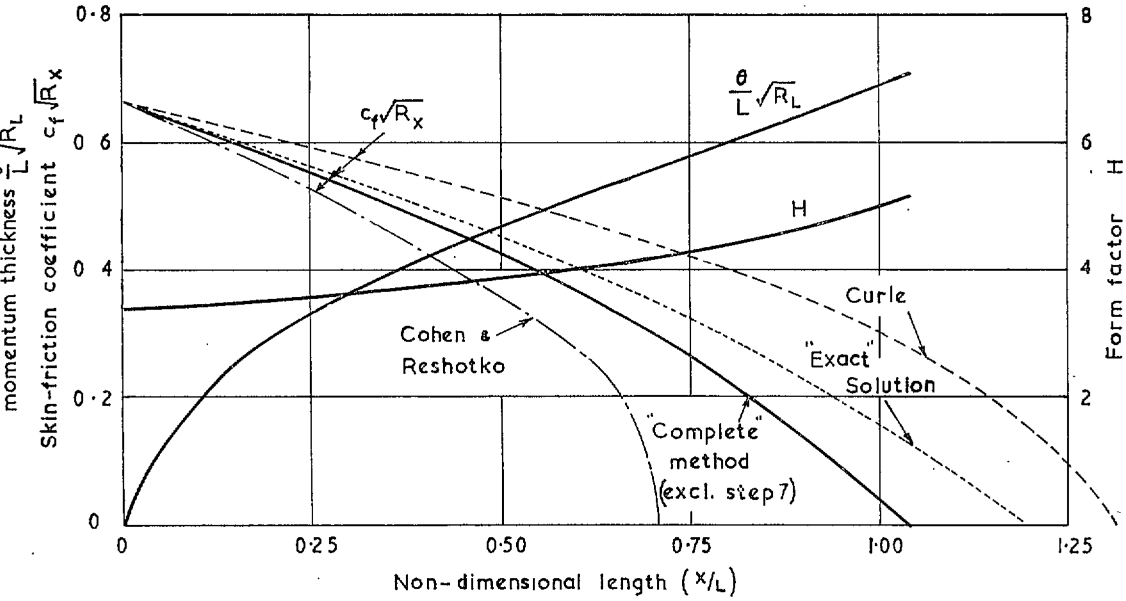

FIG. 13. Comparison of approximate methods, adverse gradient case; $p_1 = p_a(1 + x/L)$, $M_a = 2 \cdot 0$, $S_w = - 0 \cdot 762$, $(T_w = T_a)$, $\omega = \sigma = 1$.

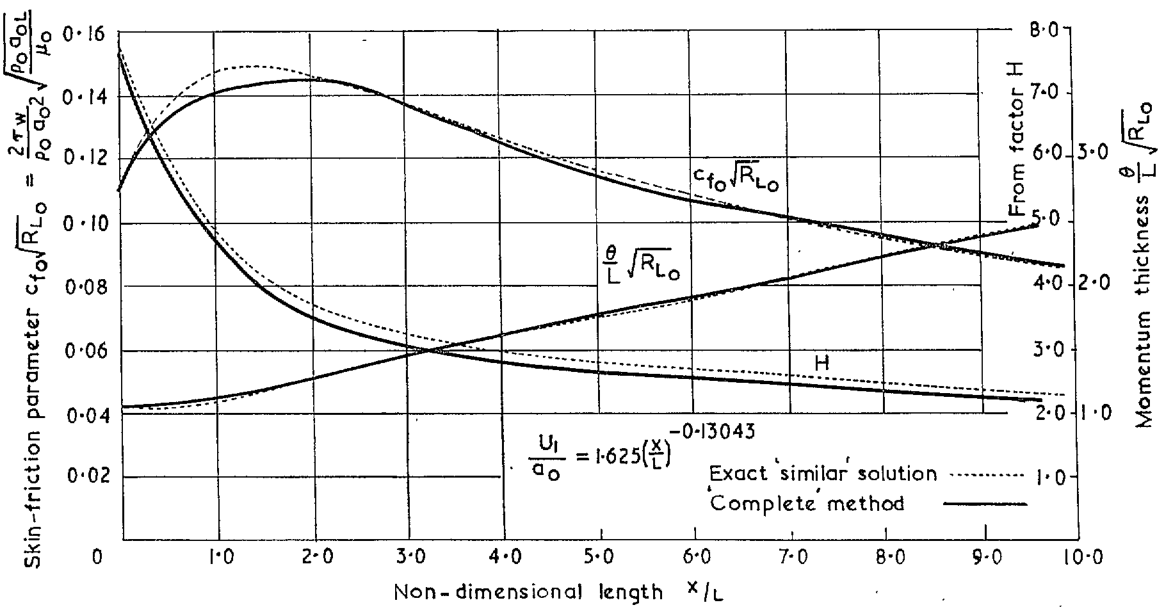

FIG. 14. Adverse pressure gradient with similar profiles.

(82878) Wt. 67/1876 K. 5 2/62 Hw.

Publications of the Aeronautical Research Council

ANNUAL TECHNICAL REPORTS OF THE AERONAUTICAL RESEARCH COUNCIL (BOUND VOLUMES)

1941 Aero and Hydrodynamics, Aerofoils, Airscrews, Engines, Flutter, Stability and Control, Structures. 63*s.* (post 2*s.* 3*d.*)

1942 Vol. I. Aero and Hydrodynamics, Aerofoils, Airscrews, Engines. 75*s.* (post 2*s.* 3*d.*)
Vol. II. Noise, Parachutes, Stability and Control, Structures, Vibration, Wind Tunnels. 47*s.* 6*d.* (post 1*s.* 9*d.*)

1943 Vol. I. Aerodynamics, Aerofoils, Airscrews. 80*s.* (post 2*s.*)
Vol. II. Engines, Flutter, Materials, Parachutes, Performance, Stability and Control, Structures. 90*s.* (post 2*s.* 3*d.*)

1944 Vol. I. Aero and Hydrodynamics, Aerofoils, Aircraft, Airscrews, Controls. 84*s.* (post 2*s.* 6*d.*)
Vol. II. Flutter and Vibration, Materials, Miscellaneous, Navigation, Parachutes, Performance, Plates and Panels, Stability, Structures, Test Equipment, Wind Tunnels. 84*s.* (post 2*s.* 6*d.*)

1945 Vol. I. Aero and Hydrodynamics, Aerofoils. 130*s.* (post 3*s.*)
Vol. II. Aircraft, Airscrews, Controls. 130*s.* (post 3*s.*)
Vol. III. Flutter and Vibration, Instruments, Miscellaneous, Parachutes, Plates and Panels, Propulsion. 130*s.* (post 2*s.* 9*d.*)
Vol. IV. Stability, Structures, Wind Tunnels, Wind Tunnel Technique. 130*s.* (post 2*s.* 9*d.*)

1946 Vol. I. Accidents, Aerodynamics, Aerofoils and Hydrofoils. 168*s.* (post 3*s.* 3*d.*)
Vol. II. Airscrews, Cabin Cooling, Chemical Hazards, Controls, Flames, Flutter, Helicopters, Instruments and Instrumentation, Interference, Jets, Miscellaneous, Parachutes. 168s. (post 2*s.* 9*d.*)
Vol. III. Performance, Propulsion, Seaplanes, Stability, Structures, Wind Tunnels. 168*s.* (post 3*s.*)

1947 Vol. I. Aerodynamics, Aerofoils, Aircraft. 168*s.* (post 3*s.* 3*d.*)
Vol. II. Airscrews and Rotors, Controls, Flutter, Materials, Miscellaneous, Parachutes, Propulsion, Seaplanes, Stability, Structures, Take-off and Landing. 168*s.* (post 3*s.* 3*d.*)

Special Volumes

Vol. I. Aero and Hydrodynamics, Aerofoils, Controls, Flutter, Kites, Parachutes, Performance, Propulsion, Stability. 126*s.* (post 2*s.* 6*d.*)
Vol. II. Aero and Hydrodynamics, Aerofoils, Airscrews, Controls, Flutter, Materials, Miscellaneous, Parachutes, Propulsion, Stability, Structures. 147*s.* (post 2*s.* 6*d.*)
Vol. III. Aero and Hydrodynamics, Aerofoils, Airscrews, Controls, Flutter, Kites, Miscellaneous, Parachutes, Propulsion, Seaplanes, Stability, Structures, Test Equipment. 189*s.* (post 3*s.* 3*d.*)

Reviews of the Aeronautical Research Council

1939–48 3*s.* (post 5*d.*) 1949–54 5*s.* (post 5*d.*)

Index to all Reports and Memoranda published in the Annual Technical Reports

1909–1947 R. & M. 2600 6*s.* (post 2*d.*)

Indexes to the Reports and Memoranda of the Aeronautical Research Council

Between Nos. 2351–2449	R. & M. No. 2450	2*s.* (post 2*d.*)
Between Nos. 2451–2549	R. & M. No. 2550	2*s.* 6*d.* (post 2*d.*)
Between Nos. 2551–2649	R. & M. No. 2650	2*s.* 6*d.* (post 2*d.*)
Between Nos. 2651–2749	R. & M. No. 2750	2*s.* 6*d.* (post 2*d.*)
Between Nos. 2751–2849	R. & M. No. 2850	2*s.* 6*d.* (post 2*d.*)
Between Nos. 2851–2949	R. & M. No. 2950	3*s.* (post 2*d.*)
Between Nos. 2951–3049	R. & M. No. 3050	3*s.* 6*d.* (post 2*d.*)

HER MAJESTY'S STATIONERY OFFICE

from the addresses overleaf

R. & M. No. 3233

Printed and published by
HER MAJESTY'S STATIONERY OFFICE

To be purchased from
York House, Kingsway, London W.C.2
423 Oxford Street, London W.1
13A Castle Street, Edinburgh 2
109 St. Mary Street, Cardiff
39 King Street, Manchester 2
50 Fairfax Street, Bristol 1
35 Smallbrook, Ringway, Birmingham 5
80 Chichester Street, Belfast 1
or through any bookseller

Printed in England

R. & M. No. 3233

S.O. Code No. 23-3233